

Review

# Physiological Alterations and Nondestructive Test Methods of Crop Seed Vigor: A Comprehensive Review

Muye Xing<sup>1,2,3,4,5</sup>, Yuan Long<sup>2,3,4,5</sup>, Qingyan Wang<sup>2,3,4,5</sup>, Xi Tian<sup>2,3,4,5</sup>, Shuxiang Fan<sup>2,3,4,5</sup>, Chi Zhang<sup>2,3,4,5</sup> and Wenqian Huang<sup>2,3,4,5,\*</sup>

<sup>1</sup> School of Agricultural Engineering, Jiangsu University, Zhenjiang 212013, China

<sup>2</sup> Intelligent Equipment Research Center, Beijing Academy of Agriculture and Forestry Sciences, Beijing 100097, China

<sup>3</sup> National Research Center of Intelligent Equipment for Agriculture, Beijing 100097, China

<sup>4</sup> Key Laboratory of Agri-Informatics, Ministry of Agriculture, Beijing 100097, China

<sup>5</sup> Beijing Key Laboratory of Intelligent Equipment Technology for Agriculture, Beijing 100097, China

\* Correspondence: huangwq@nercita.org.cn

**Abstract:** Seed vigor is one of the essential contents of agricultural research. The decline of seed vigor is described as an inevitable process. Recent studies have shown that the oxidative damage caused by reactive oxygen species (ROS) is the main reason for the destruction of various chemicals in seeds and eventually evolves into seed death. The traditional vigor tests, such as the seed germination test and TTC staining, are commonly used to assess seed vigor. However, these methods often need a large number of experimental samples, which will bring a waste of seed resources. At present, many new methods that are fast and nondestructive to seeds, such as vibrational spectroscopic techniques, have been used to test seed vigor and have achieved convincing results. This paper is aimed at analyzing the microchanges of seed-vigor decline, summarizing the performance of current seed-vigor test methods, and hoping to provide a new idea for the nondestructive testing of a single seed vigor by combining the physiological alterations of seeds with chemometrics algorithms.

**Keywords:** physiological factors; novel test; mechanism



**Citation:** Xing, M.; Long, Y.; Wang, Q.; Tian, X.; Fan, S.; Zhang, C.; Huang, W. Physiological Alterations and Nondestructive Test Methods of Crop Seed Vigor: A Comprehensive Review. *Agriculture* **2023**, *13*, 527. <https://doi.org/10.3390/agriculture13030527>

Academic Editors: Arthur Novikov, Clíssia Barboza Mastrangelo and Paweł Tylek

Received: 1 February 2023

Revised: 20 February 2023

Accepted: 20 February 2023

Published: 22 February 2023



**Copyright:** © 2023 by the authors. Licensee MDPI, Basel, Switzerland. This article is an open access article distributed under the terms and conditions of the Creative Commons Attribution (CC BY) license (<https://creativecommons.org/licenses/by/4.0/>).

## 1. Introduction

Seeds are the most basic production resources in agriculture [1], the most momentous and fundamental part of the life cycle of various crops, and the core of various technical measures in agricultural science. In the face of population growth and the repeated outbreak of COVID-19, the output of grain and other crops needs to be stable. The quality of seeds will have a significant impact on the yield of crops, which is often described by the potential of germination and seed vigor. Generally, the decline of seed vigor is caused by its internal regulation or the influence of the external environment [2].

Even if seeds are stored in the most appropriate state, the vigor of the seeds will slowly decline [3]. This process is often called seed aging. Existing studies have shown that reactive oxygen species (ROS) may be the culprit leading to a series of physiological alterations, reducing seed vigor and eventually causing seed death [4]. It is reported that a large number of outbreaks of ROS will attack lipids, proteins, and genes in cells and make their functions abnormal [5]. The damaged lipid in the membrane will produce lipid peroxide molecules and lead to the change of membrane permeability, which is a key event in the process of seed-vigor decline [6]. During this period, the nutrients in the membrane conducive to plant growth may penetrate into the matrix and affect the normal physiological activities of seeds [5]. Proteins play an irreplaceable role in cell function. The modification of proteins by ROS is also considered to be a representative event of oxidative damage to seeds, and this may be a type of permanent damage that cannot be repaired [6]. The direct consequence is that a large number of modified proteins accumulate and affect

the normal function of cells [7]. Genes are described as the core of seeds and are responsible for regulating their own physiological conditions according to external conditions. ROS accumulation will cause abnormal gene expression and eventually cause seed death [8]. However, the above changes seem to be unclear and confusing for researchers who are just starting to work on seed-vigor analysis. To solve this situation, this paper will briefly review the research status of physiological changes in the process of seed aging. The purpose is to explain the continuous physiological process of seed-vigor deterioration as much as possible, to discuss the causes of the loss of the ability for seeds to germinate, and to provide a biological basis for and to understand the mechanism of the nondestructive test of seed vigor.

If low-vigor seeds are used in agricultural production, abnormal seedlings or nongerminating seeds may be harvested, which will waste the manpower and financial resources of seed cultivation [3]. Reasonable and effective seed-vigor screening technology can test and eliminate low-vigor or dead seeds, so as to improve agricultural yield. The traditional seed-vigor test has the characteristics of being a simple test procedure and has stable results, high accuracy, and strong intuition, but it needs more experimental samples and will cause damage and waste. In recent years, spectral technology has attracted the attention of many scholars [9–16]. It has the unique advantages of being strongly objective, having excellent reproducibility, requiring generally no pretreatment, and being an onsite testing procedure, which makes it an indispensable technical method for product quality testing for such procedures as the seed-vigor test, seed mildew test, and so on. In particular, combined with hyperspectral imaging technology (HSI), the method of spectral integration analyzes the test data more comprehensively and brings better test results [17,18]. In addition, other methods for testing seed vigor have emerged one after another [19,20]. By and large, compared with the traditional 2,3,5-triphenyltetrazolium chloride (TTC) dyeing and germination methods, the combination of new scientific and technological means and new classification algorithms has the characteristics of being fast, simple, causing no damage to the seed structure, and achieving a quite high accuracy. In order to provide assistance to future researchers in the domain of seed-viability testing, this paper will review several seed-vigor test methods in recent years for understanding the principle of existing seed-vigor testing and exploring future trends.

Specifically, our review is divided into the following chapters. (1) We discuss physiological changes in the decline of seed vigor caused by ROS and how these changes affect seed vigor in turn. (2) We introduce the current vigor test methods for seeds in the process of aging or vigor decline. (3) We make some suggestions for the future research on seed vigor testing.

## 2. Physiological Factors Affecting Seed Vigor

The aging of seeds is an important reason for the decline of seed vigor, and this process is described as an irreversible common phenomenon that occurs after the seeds reach their highest point of maturity physiologically [21]. The decline of seed vigor includes the process of programmed cell death [22], reduction of ROS [4], lipid peroxidation [23], protein carbonylation [24], and the loss of enzyme activity [25]. The main process of ROS in the decline of seed vigor is shown in Figure 1. In seed science, seeds are usually divided into orthodox seeds and stubborn seeds according to their resistance to drying during storage [26]. Most commonly, grain seeds—for example maize (*Zea mays* L.), rice (*Oryza sativa* L.), soybeans (*Glycine max* (L.) Merr), barley (*Hordeum vulgare* L.), and wheat (*Triticum aestivum* L.)—all belong to the category of orthodox seeds [27]. Many authors believe that the physiological alterations of orthodox seeds in the process of seed aging may be the same. The ultimate impact of these physiological alterations on seeds is a decline in the vigor of seeds [27].

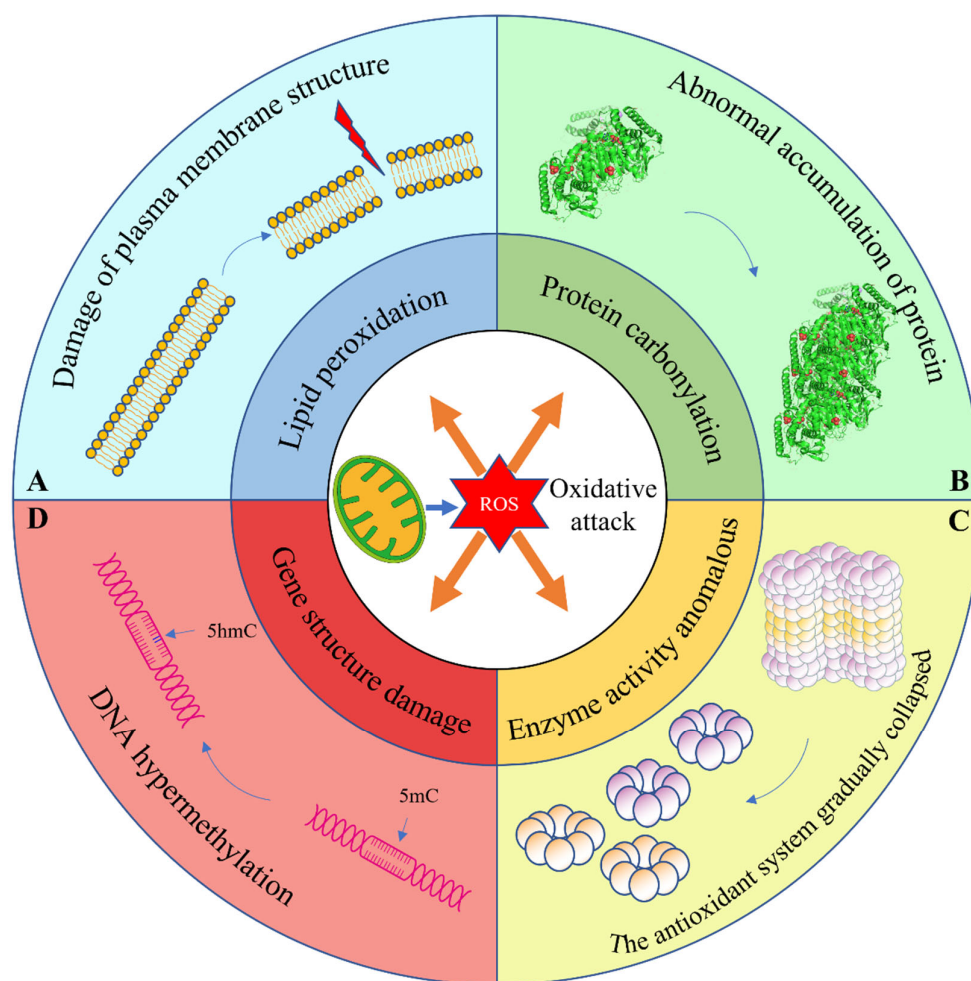


**Figure 1.** Role of ROS in the decline of seed vigor. (A) Lipids in plasma membranes are oxidized and decomposed by ROS attack. (B) Malondialdehyde (MDA) and 4-hydroxy-non-2-enal (HNE) produced by lipid peroxidation oxidize protein and damage protein function. The protein data bank (PDB) diagram of protein structure is quoted from Huang, et al. [28] PDB ID: 5NUF. (C) Abnormal enzyme activity and breakdown of the antioxidant enzyme system. (D) The gene methylation balance was broken and hypermethylation occurred, in which 5mC was methylated to 5hmC.

### 2.1. Production of Reactive Oxygen Species (ROS)

During the storage of seeds, the generation of internal ROS is mainly related to the storage conditions of seeds. ROS can be produced everywhere in seed cells, but mainly from the mitochondria in cells [29]. According to the research of Ratajczak, et al. [6], it was found that more ROS were produced in the embryo, especially in the embryonic axis of the seed. This may be closely related to the decline of seed vigor. Subsequent experiments on the protection of embryos with ROS antioxidants also confirmed this view [30]; the principle of the experiment is that the higher the concentration of antioxidants in the embryonic axis, the stronger the activity of enzyme scavengers, so as to reduce the effect of ROS on cell activity.

The production of ROS will have a destructive effect on the lipid, protein, and DNA of cells, which is the key reason for the loss of seed vigor. In addition, the decline of antioxidant enzyme activity also intensifies the decline of seed vigor. Antioxidant enzymes mainly include superoxide dismutase (SOD), catalase (CAT), peroxidase (POD), and glutathione reductase (GR), which constitute the first line of defense against ROS attack [31]. According to Yin et al. [3], the excessive accumulation of ROS will lead to the decrease or loss of ROS scavenging enzyme activity, and the first line of defense against ROS will collapse. Some scholars described the phenomenon when the balance between ROS and ROS elimination

enzymes is broken as oxidative stress [32,33]. The loss of ROS scavenging enzyme activity may even affect the rapid outbreak of ROS in the late stage of seed aging [34]. In this state, ROS will destroy the respiratory system of seeds by attacking mitochondria and cause irreversible damage to seeds.

In addition, a series of alterations, such as lipid peroxidation, protein carbonylation and Maillard reaction during the decline of seed vigor, have been confirmed to be related to the outbreak of ROS.

## 2.2. Lipid Peroxidation

When oxidative stress occurs, the dynamic balance between ROS and ROS elimination enzymes is broken, and ROS begins to erupt. At this time,  $H_2O_2$ , one of the main components of ROS, begins to attack the plasma membrane structure in the cell and form an oxygen free radical chain reaction, which is called lipid peroxidation [35]. One of the main manifestations of lipid peroxidation is the change of cell membrane permeability, which is also an important event in the process of seed-vigor decline [5,6]. According to the hypothesis made by Agmon, et al. [36] simulating the process of cell ferroptosis, the change of membrane permeability is likely to be the change of membrane characteristics caused by the deterioration after lipid peroxidation. From the perspective of molecular dynamics, the phospholipid part of the cell membrane will change in structure and characteristics after being oxidized, and the generated peroxide will have stronger binding to the hydrogen bond in water. This makes the cell membrane more hydrophilic. Therefore, it is considered that similar phenomena may also occur in the polar solution environment of the cell. When the polar solution is unbalanced in the cell of the seed, the cell may die, and the seed will lose its vigor [37].

Self-oxidation of seeds in storage environments with low water content exacerbates the process of lipid self-oxidation [38]. Lipid peroxidation can also lead to the accumulation of superoxide free radicals. As a reaction substrate, superoxide free radicals will be oxidized to  $H_2O_2$ . In fact, this increases the production of ROS. Several studies have shown that lipid autoxidation products—generally aldehydes and ketones—have been found in wheat and pea seeds [25,39]. In the aging research and analysis of corn seeds, it has been found that free fatty acids, such as linoleic acid and linolenic acid, will be oxidized and degraded into ketones, aldehydes, and alcohols in the process of lipid peroxidation. Several products, such as hexanal and nonanal, will have a negative impact on the vigor of seeds [40,41].

As a representative product of lipid peroxidation, MDA reduces the vigor of seeds by attacking membrane protein modification [42]. It was also found that the content of MDA increased with the decrease of seed vigor in other seeds [43]. Other studies on ROS-induced lipid peroxidation in plant seeds are described in the Table 1.

**Table 1.** Studies on lipid peroxidation, enzyme activity changes and gene damage during seed vigor decline.

Physiological Alternation	Type of Seed	Method of Treating Seeds	Target	Method of Analysis	Performance	Ref.
Lipid peroxidation	Almond seeds of 4 varieties	NA			MDA increase	[44]
	Bitter gourd	AA <sup>a</sup>			MDA increase	[45]
	Wheat	AA <sup>a</sup>	MDA	Spectrophotometry	No significant change (0.38–0.45)	[25]
	Karanj	NA			Positive correlation with aging days ( $r = 0.96$ )	[46]
	Pea	Drying			MDA increase	[39]
	<i>Moringa oleifera</i> oilseed	AA <sup>a</sup>			MDA increase	[43]
	Spunta	Controlled environmental conditions			MDA increased	[47]

Table 1. Cont.

Physiological Alternation	Type of Seed	Method of Treating Seeds	Target	Method of Analysis	Performance	Ref.
	<i>A. indicum</i> and <i>A. macrostachyum</i>	No special treatment			MDA increase	[48]
	<i>Brassica oleracea</i> L. and <i>Lactuca sativa</i> L.	Controlled deterioration			The change of cabbage seeds was not obvious, lettuce seeds increased significantly	[30]
	<i>Shorea robusta</i>	No special treatment	MDA; CD; HNE; FFA; LOOH; TL	Other: Spectrophotometry TL: Petroleum ether distillation	MDA: Positive correlation with aging days (r = 0.98) CD: Positive correlation with aging days (r = 0.92) HNE: Rose and then fell. FFA: Positive correlation with storage days (r = 0.96) LOOH: Positive correlation with storage days (r = 0.98) TL: Negatively correlated with storage days (r = -0.98)	[49]
	Pea	NA	POL	TCL	POL increased after seed death	[50]
	Rice	NA	Crotonaldehyde; HNE	HPLC-ESI-SIM	Increased	[51]
Enzyme activity anomalous	Rice	AA <sup>a</sup>	SOD APX CAT GR DHAR MDHAR	Spectrophotometry	APX, CAT, MDHAR: Decreased SOD, GR, DHAR: No significant change	[3]
	Beech	NA	CAT		Decreased	[6]
	Oat	AA <sup>a</sup>	SOD APX MDHAR DHAR GR		Decreased	[52]
	Karanj	NA	SOD CAT APX		Decreased	[46]
	<i>Jatropha curcas</i> L.	AA <sup>a</sup>	SOD CAT POX		Decreased after rise	[53]
	Tomato	AA <sup>a</sup>	CAT POD SOD APX GR DHAR		Decreased	[54]
	Nonheading Chinese cabbage	AA <sup>a</sup>	PGI MDH		Decreased after rise	[55]
	Bitter gourd	AA <sup>a</sup>	SOD CAT APX		Decreased	[45]
	Wheat	AA <sup>a</sup>	SOD CAT GR		Decreased	[25]
	Spunta	Controlled environmental conditions	SOD CAT GPX		Relatively stable	[46]
	<i>Moringa oleifera</i> Lam.	NA	CAT SOD APX POX		CAT, APX, SOD: Decreased POX: Increased	[21]

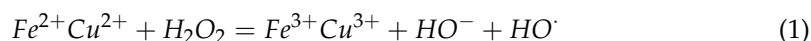
Table 1. Cont.

Physiological Alternation	Type of Seed	Method of Treating Seeds	Target	Method of Analysis	Performance	Ref.
Gene damage	<i>Brassica oleracea</i> L. and <i>Lactuca sativa</i> L.	Controlled deterioration treatment	CAT GR SOD $\alpha$ -amylase $\beta$ -1,3-glucanase	$\alpha$ -amylase: dinitrosalicylic acid, $\beta$ -1,3-glucanase: Spectrophotometry	Decreased	[30]
	Maize	NA and AA <sup>b</sup>	AOX1, ADH1, COXc, ATPase	Spectrophotometry	Upregulation of ADH1. Downregulation of COXc. ATPase and AOX1 is almost unchanged	[56]
	Oat	Controlled deterioration treatment	DEGs		Downregulation of TCA and ETC related genes. Upregulation of antioxidant enzyme related DEG	[57]
	Pea	AA <sup>b</sup>	PsAPX, PsSOD, PsGRcyt, PsGRcm	qRT-PCR	Decreased in the transcript abundance	[58]
	Rice	NA	OsAKR-1- OsAKR-3, OsALDH2-1- OsALDH2-5, OsALDH3-1- OsALDH3-5, OsALDH7		Transcript decreased	[50]
		AA <sup>a</sup>	Cu/ZnSOD1- Cu/ZnSOD3, FeSOD, MnSOD, CAT1-CAT3, APX1- APX8GR1-GR3 DHAR1, MDHAR1, MDHAR2		Downregulation of Cu/ZnSOD family genes, CAT1, CAT2, APX1, APX4, APX5, APX6, GR2, DHAR1 and MDHAR1. Upregulation of APX3, APX7, APX8, GR3.	[3]
	Beech	NA	Genomic DNA	DNA extraction and electrophoresis	DNA laddering effect	[6]
	<i>Pisum sativum</i>	Drying	PsDHN2, PsDHN3, PsSBP65, PsHSP17.7, PsHSP18.1, PsHSP18.2, PsHSP22.7, Ps2-Cys prx	qRT-PCR	Expression enhancement	[39]
	<i>Mung bean</i>	Controlled deterioration treatment	FSD1, MSD1, GST1, ZEP/ABA1, SDR, CPS1, SAM1, ACS		Downregulation of FSD1, SAM1, ACS. Upregulation of MSD1, ZEP/ABA1, SDR.	[59]
	<i>Brassica napus</i> L.	High temperature	DEGs		40 °C (83 upregulated and 37 downregulated). 60 °C (96 upregulated and 117 downregulated). 40/60 °C of heat stress exposure (88 upregulated and 158 downregulated)	[60]
	Rice	AA <sup>a</sup>	OLGLYI3		Decreased expression	[61]

NA—Natural aging; AA <sup>a</sup>—Artificial aging; AA <sup>b</sup>—Accelerated aging.

### 2.3. Abnormal Protein Modification

According to Zavadskiy, et al. [62], protein hydroxylation refers to the irreversible structural damage of proteins caused by the oxidative modification of amino acids on proteins due to the high production of highly active oxidants during cell aging. During the aging process of plant seeds, ROS, MDA, and other products of lipid peroxidation, such as HNE, play a major role in protein carbonylation. It was found that the content of malondialdehyde in some seeds was positively correlated with the performance of protein carbonylation [34,63]. MDA will have Maillard-type reaction with protein and add hydroxyl into the amino acid side chain structure of protein [64]. In living cells, hydroxyl radicals generated by Fenton reaction (1) guided by metal catalytic oxidation (MCO) attack the main chain and amino acid side chain of protein to hydroxylate the protein [65]:



Hydroxylated proteins will accumulate and aggregate, which will affect the cell vigor, such as the reduction of soluble protein content, the decrease of enzyme activity, the loosening of cell wall and so on. In the study on the aging of coix and beech seed, it was found that the content of soluble protein was negatively correlated with the degree of aging and positively correlated with the vigor of seeds [6,7]. According to another speculation of Agmon et al. [36], the loss of cell membrane characteristics may be related to the structural changes and functional impairment of proteins embedded in the cell membrane. The research results on mitochondrial membrane channel proteins of elm (*Ulmus pumila* L.) seeds also provide a basis for this hypothesis [34]. In short, seeds are rich in a variety of proteins. The irreversible oxidation of proteins by ROS and its indirect products will have an irreparable impact on the vigor of seeds.

### 2.4. Anomalous Enzyme Activity

One of the causes of seed aging is the decline or loss of enzyme activity in organisms, which is related to the attack of ROS and its indirect products. As the main role, enzymes play a positive role in seed growth. At present, the changes of enzyme activity during seed aging are mainly aimed at antioxidant enzymes and germination enzymes. Antioxidant enzymes are the main force to prevent ROS from attacking seed cells. Among them, SOD, which is commonly used to study and analyze the changes of enzyme activity during seed aging, will catalyze free radicals ( $O^{\cdot}$ ) to produce stable  $O_2$  and  $H_2O_2$ , and then decompose into water and  $O_2$  under the action of CAT or POD, so as to avoid the harm of free radicals to seed cells [66].

Due to improper storage methods (long storage time or serious dehydration in the storage environment), ROS will be produced and accumulated in excess. The dynamic balance between ROS and antioxidant enzymes is broken, the activity of antioxidant enzymes is reduced, oxidative stress occurs, and a large number of ROS outbreaks affect seed vigor [67]. The research on karanj (*Pongamia pinnata*) shows that the contents of  $O^{\cdot}$  and  $H_2O_2$  are negatively correlated with seed water content and positively correlated with seed storage time. The activity of antioxidant enzymes is positively correlated with the water content of seeds [52]. Similar phenomena have also occurred in elm and beech seeds [6,34], but it is not particularly obvious in wheat seeds [25], indicating that the relationship between antioxidant enzyme activity and seed aging may also be related to species.

In the process of seed growth, the activity of germination enzyme also decreased in the process of seed aging. In the controlled deterioration treatment of cabbage and lettuce seeds, it was found that the content of  $\alpha$ -amylase and  $\beta$ -1,3-glucanase decreased [30], and the loss of activity was also found in low-vigor rice seeds [68]. Other changes in enzyme activity are described in the Table 1.

### 2.5. Gene Damage

As a genetic structure, DNA will constantly change to meet the requirements of the environment. The outbreak of ROS will damage DNA and RNA. Hydroxyl radicals ( $\cdot\text{OH}$ ) react with base to produce free radical intermediates. At present, the most common form of damage is DNA damage caused by guanine (G) oxidation product 7,8-dihydro-8-oxo-guanine (8-oxo-G), which destroys the due principle of base complementarity [69]. This form of damage is expected to destroy 103 cells per day in normal tissues [70]. DNA methylation plays an important role in the process of seed development. Generally, methyl ( $\text{CH}_3$ -) is added to the designated position of DNA, which usually occurs in the process of DNA replication and maintains the steady-state balance through DNA demethylation [71]. There is evidence that the outbreak of  $\text{H}_2\text{O}_2$  in ROS will break this balance, which shows that 5-methylcytosine (5-mC) is oxidized to 5-hydroxymethylcytosine (5-hmC). This change tilts the above balance towards DNA methylation, resulting in DNA hypermethylation [8]. DNA hypermethylation can aggravate oxidative stress and accelerate apoptosis [72].

Evidence of DNA damage caused by ROS was found in the study of Brinjal (*Solanum melongena* L.) seeds. The results showed that when the content of ROS reached 11.84AU, the damage of the DNA tail was low (0.6%), and when the content of ROS reached 23.37AU, the damage of the DNA tail would reach 11.08%. In particular, some genes, such as OGG1 and PCNA, which repair DNA damage caused by 8-oxo-G or genes that regulate the expression of antioxidant enzymes such as CAT1 and ROS, show strong correlation or indirect strong correlation [73].

Recent studies have found that reactive carbonyl substances (RCS), an indirect product of ROS, such as crotonaldehyde, can damage RNA in rice seeds, which are mainly responsible for genes encoding carbonyl scavenging enzymes. The results showed that the expression ability of OsALDH2-2, OsALDH2-5, and OsAKR1 genes decreased by about 90%, 71%, and 43.5%, respectively, after aging treatment of rice seeds for about one year. The transcription levels of other ALDH family genes, such as OsALDH2-1 or OsALDH3-5, did not change significantly, and a negative correlation with seed vigor was even found in the analysis of OsALDH3-1. This may be due to the high resistance of these genes to ROS and its indirect products [50].

In addition, we found similar phenomena in studies on peas, Arabidopsis and beech [6,39,74]. In conclusion, the damage of ROS and its products to genes is fatal to seeds. During the storage of seeds, genes are the key to the seed's regulation and adaptation to the storage environment. Destructive gene damage will give incorrect instructions to the subsequent response of the seed to the environment and produce a series of continuous errors in the process of replication, transcription, and modification, which will eventually lead to the death of the seed. Several studies on gene expression during the decline of seed vigor are briefly introduced in Table 1.

### 2.6. Destruction of Organelle Structure

The explosion of ROS in stored seeds and the destruction of organelles are also one of the reasons for the loss of seed vigor. The main production site of ROS is mitochondria, which is responsible for cell respiration and energy supply for seeds. Therefore, it is also named "powerhouse". It is one of the organelles most sensitive to cell damage. When ROS accumulate in large quantities, mitochondria usually swell, aggregate, and suffer a collapse of the inner membrane or a blurred dissipation of mitochondrial outline; in severe cases, mitochondria may even be broken down [34,55]. This may be caused by ROS attacking mitochondrial membrane structure. Another interesting phenomenon was found in the study of pea seeds. There is a certain relationship between the integrity of mitochondrial inner membrane (IMM) and the vigor of seeds [75]. This conclusion resonates with the function of mitochondrial crest to a certain extent.

In addition to mitochondria, other organelles in seeds such as proteomes, adiposomes, and endoplasmic reticulum also changed due to the influence of ROS [55]. The nucleus is the largest and most important cell structure in eukaryotic cells. It is the main place for the

storage, replication, and transcription of genetic information in cells. According to recent studies, ROS can cause disorder or even destruction of the morphology of the nucleus and nuclear membrane, obvious matrix cavity, and chromosome breakage [76–78]. This may be caused by the damage and degradation of cell membrane and cell wall and the massive outbreak of ROS attacking the nucleolus.

Various organelles in seeds are tools to maintain the vigor of seeds during storage. The burst of ROS will damage various organelles, affect the working efficiency of organelles, and finally bring irreparable decline of vigor to seeds. However, at present, the interaction between various organelles affected by ROS is not clear, and the details of the competitive relationship between self-healing and passive destruction of various organelles after being attacked by ROS are unknown. We also hope that more scholars can discuss these in this regard in the future.

In conclusion, the decline of seed vigor is closely related to the changes of chemical composition and microstructure in seeds, such as lipid decomposition, protein carbonylation and mitochondrial structure changes. These changes provide a theoretical basis for the existing nondestructive testing of seed vigor. At present, these microchanges of seeds during storage can be detected by nondestructive methods, which can be used for qualitative and quantitative analysis of the vigor of a large-scale seed. On the other hand, understanding the seed vigor under various physiological conditions and chemical composition levels will also help us to further clarify the principle of the biological changes of seed-vigor decline. We will discuss these in the following sections.

### 3. The Relationship between Spectrum and Chemical

Molecular spectrum test technology is a method that reflects the structural information inside the molecule through the spectrum generated by the transition between molecular vibration energy levels or rotational energy levels, determines the molecular moment of inertia, molecular bond length, bond strength, and dissociation energy, and finally realizes the qualitative and quantitative test of chemical composition information in the target. Common spectral analysis technology, including near-infrared spectroscopy (NIR), visible near-infrared spectroscopy (VIS-NIR), short wave infrared spectroscopy (SWIR), and Raman spectroscopy, has been widely used in the research for analyzing agricultural products and testing seed vigor because it has the advantages of causing no damage to the tested object, requires only a fast test, carries low risk, and is environmentally friendly.

In the spectrum, different chemical composition in the sample will appear in different bands. In the common studies of analyzing seed vigor by spectrum, chemicals including proteins, carbohydrates, and lipids, which ensure the normal operation of seed life activities, are mainly analyzed. The characteristic groups of these chemical composition ( $-\text{CH}_3$ ,  $-\text{COOH}$ ,  $-\text{OH}$ , amides, and carbonyl), will leave marks in the spectrum. For example, amides will show characteristics in the NIR spectrum of  $7400\text{--}6540\text{ cm}^{-1}$  (molar absorptivity 0.7),  $5160\text{--}5060\text{ cm}^{-1}$  (molar absorptivity 3.0),  $5040\text{--}4990\text{ cm}^{-1}$  (molar absorptivity 0.5), which is related to the overtone of N-H stretch, second overtone of  $\text{C}=\text{O}$  stretch, second overtone of N-H deformation, and combination of  $\text{C}=\text{O}$  and N-H. Refer to section III of *Lange's Handbook of Chemistry (16th Edition)* [79] for more details.

As for the close relationship between seed vigor and spectrum, several research papers have reported the quantitative detection of seed vigor by using spectroscopy technology. Changes caused by seed aging (ROS accumulation, etc.) will affect the optical properties of seeds [80]. Fan et al. [9] used SPA to select nine optimal wavelengths between 1265 and 2168 nm to obtain a vigor classification model. These spectral regions are respectively related to the overtones generated by stretching vibration at C-H, O-H, N-H, and  $\text{C}=\text{O}$ , and represent the changes of protein, starch, and water. In the study of heat-damaged and artificially treated seeds, Wang et al. [81] showed absorption peaks at 1000, 1200, 1400, and 1700 nm on the original spectra, which respectively represent the content of carbohydrate, lipid and protein in corn seeds. In addition, the reflectance of the treated seeds in the spectrum is also significantly different from that of the original seeds, which indicates the

change of chemical components in the seeds during treatment. Low temperature will cause forest damage to seeds, which will lead to cytoplasmic dehydration and protein damage. In the study of detecting frozen seeds, Jia et al. [82] found that the two spectral regions of 1500 to 1700 nm and 1800 to 2100 nm in the spectral have major contributions to the vigor test model. These regions are related to the overtones produced by C-H, O-H, and N-H, and indicate the changes of chemical substances, such as proteins. Satisfying results were also obtained in the experiment of identifying normal seeds and freeze-damaged seeds by the above model. Other studies on spectral characteristics and corresponding compounds in seed vigor analysis are shown in Table 2.

**Table 2.** Studies on spectral characteristics and corresponding compounds in seed vigor analysis.

Type of Spectral	Material	Object	Band	Remarks	Ref.
NIR	Wheat	Protein, water, and starch	1200–2400 nm	Peak 1 (1265 nm, 1272 nm and 1278 nm,): Related to the starch and protein. Peak 2 (1912 nm and 2168 nm): Related to the protein. Peak 3 (2027 nm): Related to the starch.	[9]
NIR	Maize	Protein, carbohydrate, and water	1000–2400 nm	Peak 1 (1180 nm and 1420 nm): Second overtone of C-H stretching. Peak 2 (1700 nm and 1748 nm): Overtone of C-H stretching. Peak 3 (1918 nm): Related to the carbohydrate. Peak 4 (2035 nm): Related to the protein, water and starch. Peak 5 (2058 nm): Overtone of N-H stretching. Peak 6 (2275 nm): Overtone of O-H stretching.	[83]
SWIR	Maize	Starch, lipid, cellulose, protein	1100–1600 nm	Peak 1 (1220–1230 nm): Second overtone of C-H stretching (starch, lipid, cellulose). Peak 2 (1560–1570 nm): First overtone of N-H stretching (protein).	[84]
NIR-HSI	Rice	Protein	900–1700 nm	Peak 1 (1000 nm): Second overtone of N-H stretching (protein). Peak 2 (1200 nm): Second overtone of C-H stretching. Peak 3 (1400 nm): First overtone of O-H stretching.	[85]
HSI	Maize	Starch. Lipid, protein, cellulose, sugar	1000–2200 nm	Peak 1 (1100–1300 nm): Second overtone of C-H stretching (starch). Peak 2 (1450 nm): First overtone of O-H stretching (starch and lipid). Peak 3 (1700–1750 nm): Second overtone of C-H stretching (protein, starch, and lipid). Peak 4 (1800–2250 nm): Related to the protein, cellulose, and sugar.	[86]
HSI	Wheat	Protein, starch, lipid	949–1638 nm	Peak 1 (1030.9 nm and 1047.9 nm): Third overtone of N-H stretching (protein). Peak 2 (1152.4 nm and 1334.9 nm): Second overtone of C-H stretching (starch). Peak 3 (1413.3 nm and 1529.6 nm): First overtone of O-H stretching (starch and lipid).	[87]

Table 2. Cont.

Type of Spectral	Material	Object	Band	Remarks	Ref.
Raman	Maize	Protein, starch, lipid, cellulose	170–3200 $\text{cm}^{-1}$	Peak 1 (964 $\text{cm}^{-1}$ ): Related to the cellulose. Peak 2 (1660 $\text{cm}^{-1}$ ): Related to the protein. Peak 3 (2800–3000 $\text{cm}^{-1}$ ): Related to the lipid.	[83]
Raman	Pepper	Protein, carbohydrate	150–1800 $\text{cm}^{-1}$	Peak 1 (1090 $\text{cm}^{-1}$ ): Overtone of -CO stretching. Peak 2 (1154 $\text{cm}^{-1}$ ): Overtone of C-C stretching. Peak 3 (1263 $\text{cm}^{-1}$ ): Overtone of =CH stretching. Peak 4 (1440 $\text{cm}^{-1}$ ): Overtone of =CH <sub>2</sub> stretching. Peak 5 (1520 $\text{cm}^{-1}$ ): Overtone of C=C stretching.	[88]
FI-NIR	Maize	Protein, starch, and carbohydrate	1110–2500 nm	Peak 1 (1500–1700 nm) and Peak 2 (1800–2100 nm): Overtone of C-H, O-H and N-H stretching.	[82]
Vis-NIR	Maize	Protein, starch, lipid	500–1100 nm. 1000–1850 nm	Peak 1 (750 nm): Third overtone of O-H stretching. Peak 2 (800 nm): Third overtone of N-H stretching. Peak 3 (900 nm): Third overtone of C-H stretching. Peak 4 (1100 nm): Second overtone of C-H stretching.	[81]

#### 4. Current Testing Methods for Seed Vigor

Testing seed vigor is the key to ensure that high-quality seeds flow into agricultural production and plays a vital role in the complete chain of modern agricultural production. Early seed-vigor test methods include the standard germination test, conductivity test, and TTC staining. The standard germination test is a method by which to directly simulate the germination behavior of seeds to test the vigor. During seed germination, the germination performance of seeds (such as length, abnormal rate and germination rate) is tested to analyze the vigor of seeds. This usually takes at least a week. Germination rate is a phenotypic trait that describes seed viability. It is the result of comprehensive expression of many genes and a series of environmental effects. However, at the biochemical and molecular levels, it is difficult to find a biomarker that has a correlation with or can respond to the germination rate. The conductivity test is a method by which to test seed vigor by testing the electrolyte of seed leaching solution. It was first proposed in 1925 and developed to mature use in 1976 [89]. The principle of the conductivity test is related to the damage of the cell membrane, because the cell membrane of low-vigor seed is damaged to a large extent and difficult to repair itself. High-vigor seeds are the opposite. Indigo carmine is used early to detect seed vigor; live seeds are usually not stained, whereas dead seeds produce a very strong spot [90]. Similar to indigo carmine, TTC staining is also a test method for seed vigor. It was listed in the *International Rules for Seed Testing* by the International Seed Testing Association (ISTA) as early as 1953. It is a recognized simple and effective method for vigor testing. Generally, it takes tens of minutes or one day (depending on the seed type and the environmental conditions of the experiment) [34,91,92]. The principle is that the seed dehydrogenase is positively correlated with the seed vigor. This enzyme can reduce TTC to red 1,3,5-triphenylformazan (TPF), so as to intuitively judge whether the seeds are alive. It is reported that malate dehydrogenase (MDH), cytochrome c reductase, succinate dehydrogenase (SDH), and some enzymes involved in cellular information transmission system may be members of TTC reductase family [93]. The specific names of these enzymes

have not been completely checked in the current research. In a word, as an internationally recognized method, TTC staining has the advantages of simplicity and rapidity (compared with standard germination experiments), but it is not a method that meets the current requirements of large-scale seed-vigor tests because of its destructive effect to seeds. In the end, it is necessary to find a nondestructive method by which to judge whether a single seed is alive or dead. With the progress of current science, some optical methods that are faster, more convenient, and nondestructive have emerged rapidly in place of conventional methods.

#### 4.1. Vibrational Spectroscopic Techniques

As early as 1978, American scholars analyzed the water content of single corn seeds by the NIRS method [94]. Subsequently, studies on the use of NIR to analyze the information of useful components, such as oil content, starch content, and the protein quality of corn seeds also appeared one after another [95]. This laid a solid theoretical foundation for the later study of seed vigor.

In recent years, more studies emerged on the establishment of the model of seed-vigor identification through vibration spectrum technology combined with statistical analysis theory, and the model accuracy of the seed-vigor test also achieved gratifying results, especially in screening the seeds that have been damaged by heat or have lost their vigor after artificial aging treatment. In 2012, Esteve Agelet et al. [96] used NIRS to test the vigor of heat-damaged seeds by combining four statistical models: partial least squares analysis (PLS-DA), similarity classification (SIMCA), minimum support vector machine (LS-SVM), and K-NN, with the highest accuracy being 99%. Subsequently, Ambrose et al. [83] used FI-NIR, and Raman spectroscopy combined with the PLS-DA model. In the test of white corn, yellow corn, and purple corn, the accuracy of the training set and verification set was more than 95% (Figure 2B). With the maturity of spectral analysis technology and the gradual improvement of statistical models, recent similar studies have also produced results with similar conclusions or higher accuracy [9,81,97,98].

Furthermore, the research on the analysis of seed vigor by vibration spectrum analysis technology combined with visual technology has also emerged. Among them, the commonly used visual technology is hyperspectral imaging technology (HSI). Generally, the image with spectral resolution of  $10^{-2}\lambda$  is called hyperspectral imaging technology, which is a new way to perfectly combine the traditional two-dimensional technology and spectral analysis technology. It not only has the characteristics of fast, efficient, and real-time analysis of traditional spectral technology, but also has the advantages of intuitive image, good reproducibility, and high flexibility. It realizes the comprehensive analysis of samples from multiple angles. HSI has appeared in the test of seed vigor for the first time since 2016. Ambrose et al. [17] obtained more than a 95.6% accuracy in the training set and verification set of white corn with vis NIR-HSI in the wavelength range of 400–1000 nm and SWIR-HSI in the wavelength range of 1000–2500 nm combined with PLS-DA model, but the results obtained in the test of yellow corn and purple corn are not satisfactory. With the continuous development of relevant technologies, there has been some research on the analysis of seeds combined with deep learning technology (DL), including work on convolutional neural networks and the continuous projection algorithm [18,99,100], which has achieved some exciting results. The classification accuracy has reached 83.3% [83], 100% [84] (Figure 2C), and 99.35% [86] (Figure 2A) in corn seeds, and 95% [1], 99.2% [98], and 99.93% [87] in other seeds. Table 3 shows some studies using spectroscopy or spectral imaging technology in the seed-vigor test.

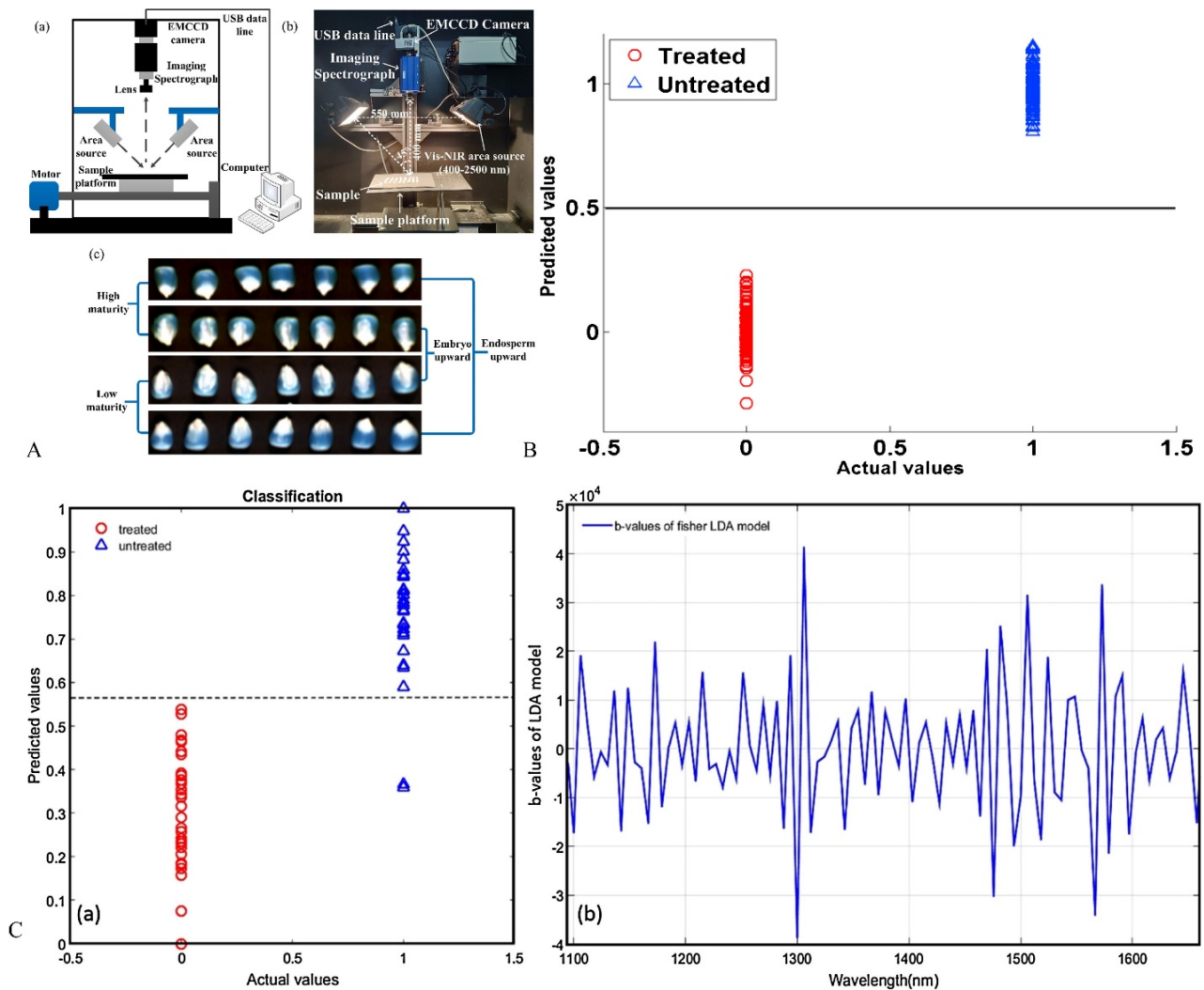


**Figure 2.** (A). NIR-HSI acquisition equipment of Wang, et al. (B). Ambrose, et al. used FT-NIR spectra of PLS-DA model to classify maize seeds. (C). Classification (a) and  $\beta$ -values (b) of LDA model by Wakholi, et al.

**Table 3.** Application and results of spectral analysis and related technology in seed-vigor research.

Type of Seed	Preparation	Spectral Analysis Technology	Analysis Model	Classification Accuracy	Ref.
Maize	Microwave treatment	NIR	PLS-DA	100%	[97]
	Artificial aging	NIR, Vis-NIR	PLS-DA; (500–1100 nm and 1000–1800 nm) CARS-PLS-DA	98.7%	[81]
Maize (white, yellow, and purple corn)	Microwave treatment	FI-NIR, Raman	PLS-DA	100%	[83]
		Vis-NIR HSI, SWIR HSI	PLS-DA	97.6%	[17]

Table 3. Cont.

Type of Seed	Preparation	Spectral Analysis Technology	Analysis Model	Classification Accuracy	Ref.
Corn	Microwave treatment and frost treatment	NIR	PLS-DA. SIMCA. LS-SVM. K-NN	99.0%	[96]
Maize	Frost treatment	NIR	PCA-OLDA or PLS-OLDA to extract spectral feature SVM, BPR, MD	99%	[82]
Corn (yellow dent corn, white dent corn, and purple flint corn)	Microwave treatment	SWIR-HSI	LDA, PLS-DA, SVM	100%	[84]
Maize	Artificial aging	ATR-FITR	PLS-DA	85%	[41]
Maize (Huanong 101)	Artificial aging	HSI	SVM. ELM. DCNN	100%	[101]
Maize (Deyu 977)	Frost damage	Vis-NIR-HSI	KNN. SVM. ELM. DCNN	100%	[102]
Maize1 (101101) and Mazie2 (7879)	Artificial aging	HSI	SVM	100%	[103]
Maize (Zhengdan 958)	Maturity division	NIR-HSI	PLS-DA. DT. AddBoost	99.35%	[86]
Retinispora (Hinoki cypress)	Not mentioned (may be natural mold infection)	FI-NIR	PLS-DA. VIP-PLS-DA	99.2%	[98]
Japanese mustard spinach ( <i>Brassica rapa</i> var. <i>perviridis</i> )	Storage for one year	NIR-HSI	CNN	-	[99]
Wheat (Luyuan 502)	Artificial aging	Vis-NIR-HSI. SWIR-HSI	PLS-R. SPA-PLS-R. PLS-R-RC	94.8%	[1]
Rice (Zhongzao39, Zhongzao 8, Y liangyou2)	Storage for 5–7 years	NIR-HSI	LR; SVM; CNN; PCA-LR; PCA-SVM; PCA-CNN	86.67%	[85]
Rice (Yanfeng)	Frost damage	NIR-HSI	DT; KNN; SVM; DF	99.93%	[87]
Wheat (Xinong 979, Xinong 20, Zhengmai 366, Xinmai 26, Zhoumai 26 and Chinese Spring)	Artificial aging	NIR	PCA/SPA + SVM/ELM/RF/AdaBoost	92.2%	[9]

The molecular vibration spectroscopy technology has made rapid development in agricultural research, especially in monitoring seed vigor, and achieved remarkable results. However, molecular spectroscopy technology still has some limitations. For example, it is difficult to achieve high-precision analysis in large-scale tests of NIR-HSI [99]. The obtained model is generally only applicable to the studied species, and more research is needed for other members of the same family [98]. The FI-NIR spectrum needs a long detection

time and a large number of manual operations for single-seed analysis, which limits its prospects for use on an industrial scale [83]. In addition, the detection temperature, sample properties, system vibration, and imperfect lighting may produce noise in the process of data collection, affecting the accuracy of the model [84]. With the development of optics, computer science, data processing technology, information transmission technology, and other related technologies, we believe that molecular spectral vibration technology will bring us more accurate and efficient performance in the future.

#### 4.2. Biological Speckle Laser

In 1975, when the British scholar Dainty [104] used lasers to irradiate objects, he found a surprising phenomenon: when one irradiates objects with highly coherent lasers, one will get an image composed of special particles with chaotic arrangement and irregular combination. The phenomenon formed in this way is called “laser speckle”. In essence, the laser speckle belongs to an optical imaging technology. Therefore, it also has the advantages of noncontact, no damage and fast image generation. However, due to its chaotic imaging, the results can only be described by statistical theory. Since its discovery, laser speckle, especially the biospeckle laser, has been effectively used in the test of fungal infection during seed storage [105], damage during seed germination [106], identification of fruit or vegetable frostbite [107], analysis, and understanding of human erythrocyte dynamics [108].

In the test of seed vigor, researchers have observed the biospeckle phenomenon caused by various physiological processes in seeds [109]. In 2003, Braga, et al. [110] prepared viable and nonviable bean seeds in advance, and successfully found their difference by using the biospeckle laser. In 2005, some scholars bisected corn seeds along the embryo axis and analyzed the seed vigor through biospeckle laser phenomenon [111]. In order to make the obtained image more direct, the concept of wavelet entropy (WE) was introduced to grade the gray area of the image according to the weight to obtain the high-activity area and low activity area of the seed. Thus, the image is reasonably explained and described. One explanation for this approach is that the presence of water in nonviable tissue. Finally, the TTC staining method commonly used in agricultural engineering is used to verify the rationality of WE-BSL method. The advantage of biospeckle laser is that the results of TTC staining for 24–48 h can be obtained in approximately one hour, which greatly improves the efficiency. With the updating of related technologies, researchers have found a faster method. Using fuzzy granularity to analyze the activity distribution area of seeds can be realized in only tens of milliseconds [112]. Then, Braga et al. [113] analyzed the homogeneous region of maize seed bisection through the method proposed by Fuji. They calculated the normalized symbiosis matrix constructed by time history speckle pattern (THSP) by using Formula (2), and finally numerically described the image by using the moment of inertia calculated by Formula (3), obtaining the same conclusion as previous scholars, and confirming the theory of biospeckle laser test of seed vigor. We have

$$COM_{ij} = \frac{COM_{ij}}{\sum_i N_{ij}} \quad (2)$$

$$IM = \sum_{ij} COM_{ij}(i - j)^2 \quad (3)$$

In terms of screening seed vigor, biospeckle laser seems to still be in its infancy, but encouraging results have been obtained [109,114,115], especially the impact of seed-tissue moisture on the measurement results; that is, whether the initial water content of seeds will affect seed germination [116]. This kind of research undoubtedly lays a foundation for the test of seed vigor by biospeckle laser, because in the process of seedling raising, the content of initial water will participate in part of the physiological process of seed germination. In recent years, several consecutive studies have shown good performance, which shows that the biospeckle laser has great applicability in testing seed vigor. Table 4 shows the

details and conclusions of several studies on the application of biospeckle laser in testing seed vigor.

**Table 4.** Performance of biospeckle laser and other method in seed-vigor research.

Method	Type of Seed	Preparation	Statistical Theory	Performance	Ref.
Biospeckle laser	Bean	Control moisture content. Prepare viable and nonviable seeds	COM-IM. GD;	Speckle can be used to distinguish the vigor of seeds	[110]
	Maize	Imbibition and bisection	WE	The distribution area of maize seed vigor was found	[111]
	Maize		Gr		[112]
	Maize		IM		[113]
	Maize and bean	Maize: Not mentioned Bean: dead and live seeds with different water content	Fuji; Entropy; IM	The distribution area of maize seed vigor was found and different manifestations of obtaining dead seeds and live seeds	[117]
	Coffee bean ( <i>Coffea arabica</i> L.)	Not mentioned	STD biospeckle index	Accuracy: 87.5%	[115]
	Chickpea ( <i>Cicer arietinum</i> L.)	Water treatment and chemical treatment	MSF-BA	BA and GR were positively correlated ( $R = 0.88, p < 0.01$ ) and negatively correlated with MGT ( $r = -0.92, p < 0.01$ )	[109]
	Bean	Disinfect and dry	FTHSP + COM + AVD	BA was positively correlated with the initial water content of seeds (0.97–0.99) and related to seed germination.	[116]
	Soybean [ <i>Glycine max</i> (L.) Merrill]	Imbibition	CNN; TL (VGG-16, VGG-19, InceptionV3, ResNet50)	Accuracy: 98.31%	[114]
	X-ray CT imaging	<i>Moringa peregrina</i> , <i>Abrus precatorius</i> , <i>Acacia tortilis</i> , <i>Acacia ehrenbergiana</i> and <i>Arthrocnemum macrostachyum</i>	No special treatment	-	High vigor seeds have clear morphology Low-vigor seeds have morphology damage
X-ray	Muskmelon seed		LDA	Accuracy: 98.9%	[119]
X-ray CT imaging	<i>Crambe abyssinica</i>		CNN	Accuracy: 95%	[19]
Biosensor (MCLA)	Pepper	Natural aging	PLS-DA	Accuracy: 88.7%	[120]
EIS	Rice (Jing Dao No. 21), Maize (Tai Gu No. 1/2), Wheat (Ze Yu No. 2)	Artificial aging	Chemiluminescence induced by MCLA	Positively correlated with TTC staining ( $r = 0.99$ )	[121]
Volatile metabolites (ethanol)	Rice	Natural aging	FLD	Accuracy: 90%	[20]
GC-IMS	Melon seed	-		Significant correlation with other germination indexes	[122]

Table 4. Cont.

Method	Type of Seed	Preparation	Statistical Theory	Performance	Ref.
X-ray CT imaging	Sweet corn	Natural aging and Artificial aging	GC-IMS-AS-PCC-VIP-PLS-R	Accuracy: 94.7%	[40]
IDS	<i>Juniperus polycarpus</i> seed				[123]
IDS	<i>Pinus patula</i> seeds	No special treatment	-	Germination rate has improved	[124]
IDS	<i>Schinus molle</i> L. seeds				[125]
Atmospheric Pressure Plasma Treatment	<i>Capsicum annuum</i> L. and <i>Trichosanthes cucumerina</i> seeds.	Stored at 25 °C for one year	-	Germination rate has improved	[126]

Biospeckle laser has become a popular diagnostic tool in the 21st century because of its simple experiment, fast acquisition, relatively stable analysis process, relatively simple algorithm. However, there is still little research on seed vigor, and the research on seed types is not extensive enough. More types of seed need to be verified by experiments. At present, scholars have made efforts to explore commercialization in this area. We also believe that this emerging method for testing seed vigor may become a possibility to test the vigor of large quantities and all types of seeds in the near future.

#### 4.3. Other Novel Means

In addition to the above common methods for evaluating seed quality, in recent years, seed experts have also demonstrated several other methods by which to test seed vigor. These methods also have the characteristics of being nondestructive, requiring a fast test, having strong objectivity, reducing human subjective influence, and being highly accurate and stable.

X-ray is a technology used to evaluate internal physical information, which has been widely used in the evaluation of seed vigor in previous years. Viable seeds have complete internal structure, a smooth seed coat, and regular endosperm shape, whereas dead seeds have an internal cavity, an endosperm deformity, seed coat damage, and so on [127]. According to these standards, an X-ray can judge whether the seeds still have the significance of putting into agriculture through the collected images [118]. Recently, the evaluation of seeds by X-ray combined with machine learning, deep learning, and a statistical model has achieved good accuracy, which proves that this method is a very promising technology in seed research [19,120].

Satisfactory results have been obtained in the test of mechanical damage, or terminal physiological death of seed. However, the disadvantage of the X-ray is also obvious. This method seems to only get the judgment of whether a seed is “alive” or “dead” because it is limited to expressing the current physical state of seeds, not microscopic chemical damage or physiological changes [119]. It is necessary to further improve the ability of X-rays to distinguish the microstructure and study the correlation between the change of microstructure and seed vigor.

Recently, analyzing the vigor of seeds according to the gas produced by seeds has become a method of great concern. This method has been used by the people for a long time. For example, when buying rice or beans, some consumers will pick up a handful and smell them to decide whether to buy or not. The carbohydrates and lipids of the seeds affected by aging will be oxidized and decomposed into odorous aldehydes and ketones, which usually have an unpleasant sour smell [128]. Compared with ordinary consumers, what seed scientists need to do is to analyze seeds that cannot be used for agricultural production in the early stage of seed vigor decline. At present, this method has been effective in the analysis of rice, corn, and melon seeds, and is expected to become a standardized measurement tool for testing seed vigor in the future [40,122,128].

Incubation, drying, and separation (IDS) is also recognized as an effective sorting technique for extracting live seeds. The principle of this technique is that seeds that have lost vigor lose water more quickly during incubation and are therefore separated. It has been reported with good results in the seed sorting of the *Juniperus polycarpus* seed (K. Koch) [123], *Pinus patula* seeds [124], and *Schinus molle* L. seeds [125]. However, the efficiency of this method seems to be dependent on the empirical nature of the researcher and the species of the seeds. Sufficient experience of the researcher is needed to set the optimal conditions for IDS. There are other methods, such as biosensor and electrical impedance spectroscopy [20,121]. However, these are not used frequently, and these types of seeds are not used widely enough. Table 4 introduces all other emerging seed test methods.

## 5. Discussion and Conclusions

Seed vigor is not only an important index by which to evaluate seed quality and production value, but also the main basis for seed classification. During the process of seed harvesting, storage, and transportation, the seed vigor will decline slowly. Developing a single seed-vigor monitoring and early warning method is a worldwide problem because the decline of seed vigor is a slow and difficult physiological activity to be observed in real time. Many studies have shown that ROS plays a vital role in the change of seed vigor. A series of physiological activities that reduce seed vigor are related to the outbreak of ROS. In fact, the seed can resist ROS attack, but it can only deal with the normal content of ROS. The excessive accumulation of ROS leads to oxidative stress, and the balance between the antioxidant system and oxidant is broken, resulting in damage to the membrane structure, nutrients, and genes of seeds. As we all know, genes are the premise for seeds to maintain normal physiological activities and the brain that regulates seeds to adapt to environmental changes. The impact of ROS on genes will make seeds misjudge the current physiological state and directly cause the death of seeds. Mitochondria are the breathing places of cells, and endoplasmic reticulum is an important synthesis base of proteins, lipids, and carbohydrate in cells. Under the influence of ROS, these organelles are also damaged. Other studies have also found that the antioxidant system will gradually collapse at this time, which makes the balance between the antioxidant system and oxidants more inclined to oxidants, and the damage to seeds is undoubtedly fatal. This series of changes are all closely related to ROS. The current researchers have proven the influence status of ROS in seed aging, but the sequence of these changes seems to be unclear. Whether the organelles in the cell have the behavior of self-defense is not clear nor is the answer to the question of how we can compensate the seeds according to the physiological changes during the decline of seed vigor, so as to prolong the seed vigor as much as possible. These issues may need require more in-depth research from scholars.

At present, in terms of seed-vigor testing, the traditional methods have the advantages of stability and simple operation. However, the result is a conclusion based on a large amount of data. The traditional methods are only for applicable random inspection other than large-scale inspection. NIR, HSI, biological speckle, X-ray CT images, and other methods have the characteristics of causing no damage, not being time-consuming, and possessing real-time analysis traits that traditional methods do not have; furthermore, all of them have achieved satisfactory results. Among these methods, vibrational spectroscopy combined with visual techniques to detect seed vigor seems to be the most effective, because it is not only fast, efficient, and provides real-time analysis, but it also allows one to analyze the changes of chemical substances inside the seeds compared to other methods, thus accurately detecting seed vigor. However, they still have limitations. NIR and HSI are difficult to establish and maintain the model, which will be unstable when mutually using different batches and types of seeds. Biospeckle has not been reported to be used among a large number of seeds, and X-ray CT images are only suitable for physical damage or good results at the end of seed-vigor decline. If a connection between the nondestructive detection and the ROS content in seeds during storage can be established, it

will more effectively help us understand the changes of seed vigor. Thus, combined with the physiological changes of seed vigor decline, it is of great significance to explore a rapid, nondestructive, and stable single seed-vigor test technology and apply it to agricultural production. The commercial use of this technology is also the duties of the development of seed science in the future.

The sufficient supply of crops is very important under the background of epidemic infestation and population growth. Seeds are at the core of agricultural production and the carriers of inherited crop resources. Seed vigor is the standard by which to evaluate seed quality. We hope that by summarizing the physiological changes in the process of seed-vigor decline and the test methods of seed vigor, we can provide seed scientists with a nondestructive, reliable, and stable seed-vigor test mechanism and finally develop a reasonable and effective early warning mechanism of seed vigor decline.

**Author Contributions:** Conceptualization, M.X. and Y.L.; methodology, W.H.; software, Q.W.; formal analysis, X.T.; investigation, S.F.; resources, C.Z.; writing—original draft preparation, M.X.; writing—review and editing, Y.L. and W.H.; supervision, W.H.; project administration, Y.L.; funding acquisition, W.H. All authors have read and agreed to the published version of the manuscript.

**Funding:** This research was funded by the financial support of China Agriculture Research System (Project No. CARS-25-07) and The APC was funded by Project No. CARS-25-07.

**Institutional Review Board Statement:** Not applicable.

**Informed Consent Statement:** Not applicable.

**Data Availability Statement:** Not applicable.

**Acknowledgments:** The authors would like to thank the National Natural Science Foundation of China (31871523), the financial support of China Agriculture Research System (Project No. CARS-25-07) and Young Elite Scientists Sponsorship Program by CAST (2019QNRC001).

**Conflicts of Interest:** The authors declare no conflict of interest.

## Nomenclature

ROS	Reactive Oxygen Species
HSI	Hyperspectral Imaging Technology
TTC	2,3,5-Triphenyltetrazolium Chloride
MDA	Malondialdehyde
HNE	4-Hydroxy-Non-2-Enal
NA	Natural Aging
AA <sup>a</sup>	Artificial Aging
AA <sup>b</sup>	Accelerated Aging
CD	Conjugated Diene
FFA	Free Fatty Acid
LOOH	Lipid Hydroperoxide
TL	Total Lipid
POL	Product Of Lipid
CAT	Catalase
SOD	Superoxide Dismutase
APX	Ascorbic Acid Peroxidase
GR	Glutathione Reductase
DHAR	Dehydroascorbic Acid Reductase
MDHAR	Monodehydroascorbate Reductase
GPX	Glutathione Peroxidase
POX	Peroxidase
PGI	Phosphohexose Isomerase
MDH	Malate Dehydrogenase
qRT-PCR	Quantitative Real-Time Polymerase Chain Reaction
TCL	Thermochemiluminescence

HPLC-ESI-SIM	High Performance Liquid Chromatography-Electrospray Ionization-Selective Ion Monitoring.
DEG	Differentially Expressed Genes
NIR	Near Infrared Spectroscopy
VIS-NIR	Visible Near-Infrared Spectroscopy
SWIR	Short Wave Infrared Spectroscopy
ISTA	International Rules for Seed Testing by the International Seed Testing Association
TPF	1,3,5-triphenylformazan
PLS-DA	Partial Least Squares Analysis
SIMCA	Similarity Classification
LS-SVM	Minimum Support Vector Machine
DL	Deep Learning Technology
K-NN	K-Nearest Neighbors
FI-NIR	Fourier Transform Infrared
CARS	Competitive Adaptive Reweighted Sampling
PLS-OLDA	Partial Least Squares-Orthogonal Linear Discriminant Analysis
SVM	Support Vector Machine
BPR	Biomimetic Pattern Recognition
MD	Mahalanobis Distance
LDA	Linear Discriminant Analysis
ATR-FITR	Attenuated Total Reflectance-Fourier Transform Infrared Spectroscopy
ELM	Extreme Learning Machine
DCNN	Deep Convolutional Neural Networks
DT	Decision Tree
VIP	Variable Importance of Projection
CNN	Convolutional Neural Networks
PLS-R	Partial Least Squares Regression
SPA	Successive Projection Algorithm
RC	Regression Coefficients
LR	Logistic Regression
DF	Deep Forests
RF	Random Forest
COM-IM	Moment of Inertia of Co-occurrence Matrix
GD	Generalized Differences
WE	Wavelet Entropy
Gr	Granularity
STD	Standard Deviation
MSF-BA	Modified structural Function-Biospeckle Activity
FTHSP	Full-Field Time History of Speckle Pattern
AVD	Absolute Value of Difference
TL	Transfer Learning
MCLA	2-methyl-6-(p-methoxyphenyl)-3,7-dihydroimidazo [1,2 $\alpha$ ] pyrazin-3-one
ELS	Electrical Impedance Spectroscopy
GC-IMS	Gas Chromatography-Ion Mobility Spectrometry.
IDS	Incubation, Drying and Separation

## References

- Zhang, T.; Fan, S.; Xiang, Y.; Zhang, S.; Wang, J.; Sun, Q. Non-destructive analysis of germination percentage, germination energy and simple vigour index on wheat seeds during storage by Vis/NIR and SWIR hyperspectral imaging. *Spectrochim. Acta Part A Mol. Biomol. Spectrosc.* **2020**, *239*, 118488. [[CrossRef](#)] [[PubMed](#)]
- Ghosh, M.; Gorain, J.; Pal, A.K.; Saha, B.; Chakraborti, P.; Avinash, B.; Pyngrupe, D.M.; Banerjee, S.; Sarkar, S. Study of seed morphology and influence of ageing and storage conditions on germination and seedling vigour of non-Basmati aromatic rice. *J. Stored Prod. Res.* **2021**, *93*, 101863. [[CrossRef](#)]
- Yin, G.; Xin, X.; Song, C.; Chen, X.; Zhang, J.; Wu, S.; Li, R.; Liu, X.; Lu, X. Activity levels and expression of antioxidant enzymes in the ascorbate–glutathione cycle in artificially aged rice seed. *Plant Physiol. Biochem.* **2014**, *80*, 1–9. [[CrossRef](#)]
- Bailly, C. Active oxygen species and antioxidants in seed biology. *Seed Sci. Res.* **2004**, *14*, 93–107. [[CrossRef](#)]
- Apel, K.; Hirt, H. REACTIVE OXYGEN SPECIES: Metabolism, Oxidative Stress, and Signal Transduction. *Annu. Rev. Plant Biol.* **2004**, *55*, 373–399. [[CrossRef](#)] [[PubMed](#)]

6. Ratajczak, E.; Małecka, A.; Bagniewska-Zadworna, A.; Kalembe, E.M. The production, localization and spreading of reactive oxygen species contributes to the low vitality of long-term stored common beech (*Fagus sylvatica* L.) seeds. *J. Plant Physiol.* **2015**, *174*, 147–156. [[CrossRef](#)]
7. Xu, M.; He, D.; Teng, H.; Chen, L.; Song, H.; Huang, Q. Physiological and proteomic analyses of coix seed aging during storage. *Food Chem.* **2018**, *260*, 82–89. [[CrossRef](#)]
8. Zhou, X.; Zhuang, Z.; Wang, W.; He, L.; Wu, H.; Cao, Y.; Pan, F.; Zhao, J.; Hu, Z.; Sekhar, C.; et al. OGG1 is essential in oxidative stress induced DNA demethylation. *Cell. Signal.* **2016**, *28*, 1163–1171. [[CrossRef](#)]
9. Fan, Y.; Ma, S.; Wu, T. Individual wheat kernels vigor assessment based on NIR spectroscopy coupled with machine learning methodologies. *Infrared Phys. Technol.* **2020**, *105*, 103213. [[CrossRef](#)]
10. Tian, X.; Zhang, C.; Li, J.; Fan, S.; Yang, Y.; Huang, W. Detection of early decay on citrus using LW-NIR hyperspectral reflectance imaging coupled with two-band ratio and improved watershed segmentation algorithm. *Food Chem.* **2021**, *360*, 130077. [[CrossRef](#)]
11. Yang, Y.; Zhao, C.; Huang, W.; Tian, X.; Fan, S.; Wang, Q.; Li, J. Optimization and compensation of models on tomato soluble solids content assessment with online Vis/NIRS diffuse transmission system. *Infrared Phys. Technol.* **2022**, *121*, 104050. [[CrossRef](#)]
12. Yang, Y.; Zhuang, H.; Yoon, S.-C.; Wang, W.; Jiang, H.; Jia, B. Rapid classification of intact chicken breast fillets by predicting principal component score of quality traits with visible/near-Infrared spectroscopy. *Food Chem.* **2018**, *244*, 184–189. [[CrossRef](#)]
13. Long, Y.; Huang, W.; Wang, Q.; Fan, S.; Tian, X. Integration of textural and spectral features of Raman hyperspectral imaging for quantitative determination of a single maize kernel mildew coupled with chemometrics. *Food Chem.* **2022**, *372*, 131246. [[CrossRef](#)] [[PubMed](#)]
14. Fan, S.; Liang, X.; Huang, W.; Zhang, V.; Pang, Q.; He, X.; Li, L.; Zhang, C. Real-time defects detection for apple sorting using NIR cameras with pruning-based YOLOV4 network. *Comput. Electron. Agric.* **2022**, *193*, 106715. [[CrossRef](#)]
15. Li, L.; Huang, W.; Wang, Z.; Liu, S.; He, X.; Fan, S. Calibration transfer between developed portable Vis/NIR devices for detection of soluble solids contents in apple. *Postharvest Biol. Technol.* **2022**, *183*, 111720. [[CrossRef](#)]
16. Fan, S.; Li, J.; Zhang, Y.; Tian, X.; Wang, Q.; He, X.; Zhang, C.; Huang, W. On line detection of defective apples using computer vision system combined with deep learning methods. *J. Food Eng.* **2020**, *286*, 110102. [[CrossRef](#)]
17. Ambrose, A.; Kandpal, L.M.; Kim, M.S.; Lee, W.-H.; Cho, B.-K. High speed measurement of corn seed viability using hyperspectral imaging. *Infrared Phys. Technol.* **2016**, *75*, 173–179. [[CrossRef](#)]
18. Pang, L.; Wang, L.; Yuan, P.; Yan, L.; Xiao, J. Rapid seed viability prediction of *Sophora japonica* by improved successive projection algorithm and hyperspectral imaging. *Infrared Phys. Technol.* **2022**, *123*, 104143. [[CrossRef](#)]
19. De Medeiros, A.D.; Bernardes, R.C.; da Silva, L.J.; de Freitas, B.A.L.; dos Santos Dias, D.C.F.; da Silva, C.B. Deep learning-based approach using X-ray images for classifying *Crambe abyssinica* seed quality. *Ind. Crops Prod.* **2021**, *164*, 113378. [[CrossRef](#)]
20. Feng, L.; Hou, T.; Wang, B.; Zhang, B. Assessment of rice seed vigour using selected frequencies of electrical impedance spectroscopy. *Biosyst. Eng.* **2021**, *209*, 53–63. [[CrossRef](#)]
21. De Melo, S.M.B.; Alves-de-Oliveira, D.F.; Souza, N.C.; Tavares-Silva, W.K.; de Macêdo, C.E.C.; Voigt, E.L. Oxidative status of *Moringa oleifera* Lam. seeds during storage. *S. Afr. J. Bot.* **2020**, *129*, 429–434. [[CrossRef](#)]
22. Hu, D.; Ma, G.; Wang, Q.; Yao, J.; Wang, Y.; Pritchard, H.; Wang, X. Spatial and temporal nature of reactive oxygen species production and programmed cell death in elm (*Ulmus pumila* L.) seeds during controlled deterioration. *Plant Cell Environ.* **2012**, *35*, 2045–2059. [[CrossRef](#)]
23. Oenel, A.; Fekete, A.; Krischke, M.; Faul, S.C.; Gresser, G.; Havaux, M.; Mueller, M.J.; Berger, S. Enzymatic and Non-Enzymatic Mechanisms Contribute to Lipid Oxidation During Seed Aging. *Plant Cell Physiol.* **2017**, *58*, 925–933. [[CrossRef](#)] [[PubMed](#)]
24. Rajjou, L.; Lovigny, Y.; Groot, S.P.C.; Belghazi, M.; Job, C.; Job, D. Proteome-Wide Characterization of Seed Aging in Arabidopsis: A Comparison between Artificial and Natural Aging Protocols. *Plant Physiol.* **2008**, *148*, 620–641. [[CrossRef](#)] [[PubMed](#)]
25. Lehner, A.; Mamadou, N.; Poels, P.; Côme, D.; Bailly, C.; Corbineau, F. Changes in soluble carbohydrates, lipid peroxidation and antioxidant enzyme activities in the embryo during ageing in wheat grains. *J. Cereal Sci.* **2008**, *47*, 555–565. [[CrossRef](#)]
26. Roberts, E. Predicting the storage life of seeds. *Seed Sci. Technol.* **1973**, *1*, 499–514.
27. Ebone, L.A.; Caverzan, A.; Chavarria, G. Physiologic alterations in orthodox seeds due to deterioration processes. *Plant Physiol. Biochem.* **2019**, *145*, 34–42. [[CrossRef](#)]
28. Huang, J.; Niazi, A.K.; Young, D.; Rosado, L.A.; Vertommen, D.; Bodra, N.; Abdelgawwad, M.R.; Vignols, F.; Wei, B.; Wahni, K.; et al. Self-protection of cytosolic malate dehydrogenase against oxidative stress in Arabidopsis. *J. Exp. Bot.* **2017**, *69*, 3491–3505. [[CrossRef](#)]
29. El-Maarouf-Bouteau, H.; Bailly, C. Oxidative signaling in seed germination and dormancy. *Plant Signal. Behav.* **2008**, *3*, 175–182. [[CrossRef](#)]
30. Adetunji, A.E.; Sershen; Varghese, B.; Pammenter, N. Effects of exogenous application of five antioxidants on vigour, viability, oxidative metabolism and germination enzymes in aged cabbage and lettuce seeds. *S. Afr. J. Bot.* **2021**, *137*, 85–97. [[CrossRef](#)]
31. Miernyk, J.A.; Johnston, M.L.; Huber, S.C.; Tovar-Méndez, A.; Hoyos, E.; Randall, D.D. Oxidation of an Adjacent Methionine Residue Inhibits Regulatory Seryl-Phosphorylation of Pyruvate Dehydrogenase. *Proteom. Insights* **2009**, *2*, PRI.S2799. [[CrossRef](#)]
32. Chandra, J.; Sershen, N.; Varghese, B.; Sahu, K. The Potential of ROS Inhibitors and Hydrated Storage in Improving the Storability of Recalcitrant *Madhuca Latifolia* Seeds. *Seed Sci. Technol.* **2019**, *47*, 33–45. [[CrossRef](#)]
33. Choudhury, F.K.; Rivero, R.M.; Blumwald, E.; Mittler, R. Reactive oxygen species, abiotic stress and stress combination. *Plant J.* **2017**, *90*, 856–867. [[CrossRef](#)] [[PubMed](#)]

34. Li, Y.; Wang, Y.; Xue, H.; Pritchard, H.W.; Wang, X. Changes in the mitochondrial protein profile due to ROS eruption during ageing of elm (*Ulmus pumila* L.) seeds. *Plant Physiol. Biochem.* **2017**, *114*, 72–87. [[CrossRef](#)]
35. Su, D.; Wang, X.; Zhang, W.; Li, P.; Tang, B. Fluorescence imaging for visualizing the bioactive molecules of lipid peroxidation within biological systems. *TrAC Trends Anal. Chem.* **2022**, *146*, 116484. [[CrossRef](#)]
36. Agmon, E.; Solon, J.; Bassereau, P.; Stockwell, B.R. Modeling the effects of lipid peroxidation during ferroptosis on membrane properties. *Sci. Rep.* **2018**, *8*, 5155. [[CrossRef](#)]
37. Wong-ekkabut, J.; Xu, Z.; Triampo, W.; Tang, I.M.; Peter Tieleman, D.; Monticelli, L. Effect of Lipid Peroxidation on the Properties of Lipid Bilayers: A Molecular Dynamics Study. *Biophys. J.* **2007**, *93*, 4225–4236. [[CrossRef](#)]
38. Leprince, O.; Atherton, N.; Deltour, R.; Hendry, C. The Involvement of Respiration in Free Radical Processes during Loss of Desiccation Tolerance in Germinating *Zea mays* L. (An Electron Paramagnetic Resonance Study). *Plant Physiol.* **1994**, *104*, 1333–1339. [[CrossRef](#)]
39. Sahu, B.; Sahu, A.K.; Sahu, A.; Naithani, S.C. Gene expression of late embryogenesis abundant proteins, small heat shock proteins and peroxiredoxin and oxidation of lipid and protein during loss and re-establishment of desiccation tolerance in *Pisum sativum* seeds. *S. Afr. J. Bot.* **2018**, *119*, 28–36. [[CrossRef](#)]
40. Zhang, T.; Ayed, C.; Fisk, I.D.; Pan, T.; Wang, J.; Yang, N.; Sun, Q. Evaluation of volatile metabolites as potential markers to predict naturally-aged seed vigour by coupling rapid analytical profiling techniques with chemometrics. *Food Chem.* **2022**, *367*, 130760. [[CrossRef](#)]
41. Andrade, G.C.; Medeiros Coelho, C.M.; Uarrota, V.G. Modelling the vigour of maize seeds submitted to artificial accelerated ageing based on ATR-FTIR data and chemometric tools (PCA, HCA and PLS-DA). *Heliyon* **2020**, *6*, e03477. [[CrossRef](#)]
42. Zhao, Y.; Tang, J.; Song, C.; Qi, S.; Lin, Q.; Cui, Y.; Ling, J.; Duan, Y. Nitric oxide alleviates chilling injury by regulating the metabolism of lipid and cell wall in cold-storage peach fruit. *Plant Physiol. Biochem.* **2021**, *169*, 63–69. [[CrossRef](#)]
43. Fotouo-M, H.; Vorster, J.; du Toit, E.S.; Robbertse, P.J. The effect of natural long-term packaging methods on antioxidant components and malondialdehyde content and seed viability *Moringa oleifera* oilseed. *S. Afr. J. Bot.* **2020**, *129*, 17–24. [[CrossRef](#)]
44. Zacheo, G.; Cappello, M.S.; Gallo, A.; Santino, A.; Cappello, A.R. Changes Associated with Post-harvest Ageing in Almond Seeds. *LWT Food Sci. Technol.* **2000**, *33*, 415–423. [[CrossRef](#)]
45. Hsu, C.C.; Chen, C.L.; Chen, J.J.; Sung, J.M. Accelerated aging-enhanced lipid peroxidation in bitter melon seeds and effects of priming and hot water soaking treatments. *Sci. Hortic.* **2003**, *98*, 201–212. [[CrossRef](#)]
46. Sahu, B.; Sahu, A.K.; Thomas, V.; Naithani, S.C. Reactive oxygen species, lipid peroxidation, protein oxidation and antioxidative enzymes in dehydrating Karanj (*Pongamia pinnata*) seeds during storage. *S. Afr. J. Bot.* **2017**, *112*, 383–390. [[CrossRef](#)]
47. Kammoun, M.; Essid, M.F.; Ksouri, F.; Rokka, V.-M.; Charfeddine, M.; Gargouri-Bouzid, R.; Nouri-Ellouz, O. Assessment of physiological age and antioxidant status of new somatic hybrid potato seeds during extended cold storage. *J. Plant Physiol.* **2020**, *254*, 153279. [[CrossRef](#)]
48. Nisar, F.; Gul, B.; Khan, M.A.; Hameed, A. Heteromorphic seeds of coastal halophytes *Arthrocnemum macrostachyum* and *A. indicum* display differential patterns of hydrogen peroxide accumulation, lipid peroxidation and antioxidant activities under increasing salinity. *Plant Physiol. Biochem.* **2019**, *144*, 58–63. [[CrossRef](#)] [[PubMed](#)]
49. Parkhey, S.; Naithani, S.C.; Keshavkant, S. ROS production and lipid catabolism in desiccating *Shorea robusta* seeds during aging. *Plant Physiol. Biochem.* **2012**, *57*, 261–267. [[CrossRef](#)] [[PubMed](#)]
50. Veselova, T.V.; Veselovsky, V.A.; Obroucheva, N.V. Deterioration mechanisms in air-dry pea seeds during early aging. *Plant Physiol. Biochem.* **2015**, *87*, 133–139. [[CrossRef](#)] [[PubMed](#)]
51. Fu, S.; Yin, G.; Xin, X.; Wu, S.; Wei, X.; Lu, X. Levels of Crotonaldehyde and 4-hydroxy-(E)-2-nonenal and Expression of Genes Encoding Carbonyl-Scavenging Enzyme at Critical Node During Rice Seed Aging. *Rice Sci.* **2018**, *25*, 152–160.
52. Xia, F.; Wang, X.; Li, M.; Mao, P. Mitochondrial structural and antioxidant system responses to aging in oat (*Avena sativa* L.) seeds with different moisture contents. *Plant Physiol. Biochem.* **2015**, *94*, 122–129. [[CrossRef](#)] [[PubMed](#)]
53. Suresh, A.; Shah, N.; Kotecha, M.; Robin, P. Evaluation of biochemical and physiological changes in seeds of *Jatropha curcas* L. Under natural aging, accelerated aging and saturated salt accelerated aging. *Sci. Hortic.* **2019**, *255*, 21–29. [[CrossRef](#)]
54. Nigam, M.; Mishra, A.P.; Salehi, B.; Kumar, M.; Sahrifi-Rad, M.; Coviello, E.; Iriti, M.; Sharifi-Rad, J. Accelerated ageing induces physiological and biochemical changes in tomato seeds involving MAPK pathways. *Sci. Hortic.* **2019**, *248*, 20–28. [[CrossRef](#)]
55. Jiang, F.L.; Bo, L.P.; Xu, J.J.; Wu, Z. Changes in respiration and structure of non-heading Chinese cabbage seeds during gradual artificial aging. *Sci. Hortic.* **2018**, *238*, 14–22. [[CrossRef](#)]
56. Chaengsakul, C.; Onwimol, D.; Kongsil, P.; Suwannarat, S. Ethanol production and mitochondrial-related gene expression of maize (*Zea mays*) seed during storage. *J. Integr. Agric.* **2019**, *18*, 2435–2445. [[CrossRef](#)]
57. Cheng, H.; Ma, X.; Jia, S.; Li, M.; Mao, P. Transcriptomic analysis reveals the changes of energy production and AsA-GSH cycle in oat embryos during seed ageing. *Plant Physiol. Biochem.* **2020**, *153*, 40–52. [[CrossRef](#)]
58. Yao, Z.; Liu, L.; Gao, F.; Rampitsch, C.; Reinecke, D.M.; Ozga, J.A.; Ayele, B.T. Developmental and seed aging mediated regulation of antioxidative genes and differential expression of proteins during pre- and post-germinative phases in pea. *J. Plant Physiol.* **2012**, *169*, 1477–1488. [[CrossRef](#)]
59. Sharma, S.N.; Maheshwari, A.; Sharma, C.; Shukla, N. Gene expression patterns regulating the seed metabolism in relation to deterioration/ageing of primed mung bean (*Vigna radiata* L.) seeds. *Plant Physiol. Biochem.* **2018**, *124*, 40–49. [[CrossRef](#)]

60. Gao, G.; Hu, J.; Zhang, X.; Zhang, F.; Li, M.; Wu, X. Transcriptome analysis reveals genes expression pattern of seed response to heat stress in *Brassica napus* L. *Oil Crop Sci.* **2021**, *6*, 87–96. [[CrossRef](#)]
61. Liu, S.; Liu, W.; Lai, J.; Liu, Q.; Zhang, W.; Chen, Z.; Gao, J.; Song, S.; Liu, J.; Xiao, Y. OsGLYI3, a glyoxalase gene expressed in rice seed, contributes to seed longevity and salt stress tolerance. *Plant Physiol. Biochem.* **2022**, *183*, 85–95. [[CrossRef](#)] [[PubMed](#)]
62. Zavadskiy, S.; Sologova, S.; Moldogazieva, N. Oxidative distress in aging and age-related diseases: Spatiotemporal dysregulation of protein oxidation and degradation. *Biochimie* **2022**, *195*, 114–134. [[CrossRef](#)] [[PubMed](#)]
63. Li, F.; Wu, X.; Wu, W. Effects of oxidative modification by malondialdehyde on the in vitro digestion properties of rice bran protein. *J. Cereal Sci.* **2021**, *97*, 103158. [[CrossRef](#)]
64. Møller, I.M.; Rogowska-Wrzesinska, A.; Rao, R.S.P. Protein carbonylation and metal-catalyzed protein oxidation in a cellular perspective. *J. Proteom.* **2011**, *74*, 2228–2242. [[CrossRef](#)]
65. Bertini, I.; Gray, H.B.; Stiefel, E.I.; Valentine, J.S. Dioxxygen reactivity and toxicity. *Biol. Inorg. Chem. Struct. React.* **2007**, 31–41.
66. Srivalli, S.; Khanna-Chopra, R. Delayed wheat flag leaf senescence due to removal of spikelets is associated with increased activities of leaf antioxidant enzymes, reduced glutathione/oxidized glutathione ratio and oxidative damage to mitochondrial proteins. *Plant Physiol. Biochem.* **2009**, *47*, 663–670. [[CrossRef](#)]
67. McDonald, M. Seed deterioration: Physiology, repair and assessment. *Seed Sci. Technol.* **1999**, *27*, 177–237.
68. Wang, Y.; Cui, Y.; Hu, G.; Wang, X.; Chen, H.; Shi, Q.; Xiang, J.; Zhang, Y.; Zhu, D.; Zhang, Y. Reduced bioactive gibberellin content in rice seeds under low temperature leads to decreased sugar consumption and low seed germination rates. *Plant Physiol. Biochem.* **2018**, *133*, 1–10. [[CrossRef](#)]
69. Van Loon, B.; Markkanen, E.; Hübscher, U. Oxygen as a friend and enemy: How to combat the mutational potential of 8-oxo-guanine. *DNA Repair* **2010**, *9*, 604–616. [[CrossRef](#)]
70. Lindahl, T.; Barnes, D.E. Repair of endogenous DNA damage. *Cold Spring Harb. Symp. Quant. Biol.* **2000**, *65*, 127–133. [[CrossRef](#)]
71. Dawlaty, M.M.; Breiling, A.; Le, T.; Barrasa, M.I.; Raddatz, G.; Gao, Q.; Powell, B.E.; Cheng, A.W.; Faull, K.F.; Lyko, F.; et al. Loss of Tet Enzymes Compromises Proper Differentiation of Embryonic Stem Cells. *Dev. Cell* **2014**, *29*, 102–111. [[CrossRef](#)] [[PubMed](#)]
72. Menezes, Y.J.R.; Silvestris, E.; Dale, B.; Elder, K. Oxidative stress and alterations in DNA methylation: Two sides of the same coin in reproduction. *Reprod. BioMed. Online* **2016**, *33*, 668–683. [[CrossRef](#)] [[PubMed](#)]
73. Kiran, K.R.; Deepika, V.B.; Swathy, P.S.; Prasad, K.; Kabekkodu, S.P.; Murali, T.S.; Satyamoorthy, K.; Muthusamy, A. ROS-dependent DNA damage and repair during germination of NaCl primed seeds. *J. Photochem. Photobiol. B Biol.* **2020**, *213*, 112050. [[CrossRef](#)] [[PubMed](#)]
74. Zhu, H.; Yang, X.; Wang, X.; Li, Q.; Guo, J.; Ma, T.; Zhao, C.; Tang, Y.; Qiao, L.; Wang, J.; et al. The sweetpotato  $\beta$ -amylase gene IbBAM1.1 enhances drought and salt stress resistance by regulating ROS homeostasis and osmotic balance. *Plant Physiol. Biochem.* **2021**, *168*, 167–176. [[CrossRef](#)]
75. Khan, A.R.; Azhar, W.; Wu, J.; Ulhassan, Z.; Salam, A.; Zaidi, S.H.R.; Yang, S.; Song, G.; Gan, Y. Ethylene participates in zinc oxide nanoparticles induced biochemical, molecular and ultrastructural changes in rice seedlings. *Ecotoxicol. Environ. Saf.* **2021**, *226*, 112844. [[CrossRef](#)]
76. Salam, A.; Khan, A.R.; Liu, L.; Yang, S.; Azhar, W.; Ulhassan, Z.; Zeeshan, M.; Wu, J.; Fan, X.; Gan, Y. Seed priming with zinc oxide nanoparticles downplayed ultrastructural damage and improved photosynthetic apparatus in maize under cobalt stress. *J. Hazard. Mater.* **2022**, *423*, 127021. [[CrossRef](#)]
77. Spanò, C.; Muccifora, S.; Ruffini Castiglione, M.; Bellani, L.; Bottega, S.; Giorgetti, L. Polystyrene nanoplastics affect seed germination, cell biology and physiology of rice seedlings in-short term treatments: Evidence of their internalization and translocation. *Plant Physiol. Biochem.* **2022**, *172*, 158–166. [[CrossRef](#)]
78. Kareem, H.A.; Hassan, M.U.; Zain, M.; Irshad, A.; Shakoob, N.; Saleem, S.; Niu, J.; Skalicky, M.; Chen, Z.; Guo, Z.; et al. Nanosized zinc oxide (n-ZnO) particles pretreatment to alfalfa seedlings alleviate heat-induced morpho-physiological and ultrastructural damages. *Environ. Pollut.* **2022**, *303*, 119069. [[CrossRef](#)]
79. Speight, J.G. *Lange's Handbook of Chemistry*; McGraw-Hill: New York, NY, USA, 2004.
80. Wu, N.; Weng, S.; Chen, J.; Xiao, Q.; Zhang, C.; He, Y. Deep convolution neural network with weighted loss to detect rice seeds vigor based on hyperspectral imaging under the sample-imbalanced condition. *Comput. Electron. Agric.* **2022**, *196*, 106850. [[CrossRef](#)]
81. Wang, Y.; Peng, Y.; Qiao, X.; Zhuang, Q. Discriminant analysis and comparison of corn seed vigor based on multiband spectrum. *Comput. Electron. Agric.* **2021**, *190*, 106444. [[CrossRef](#)]
82. Jia, S.; Yang, L.; An, D.; Liu, Z.; Yan, Y.; Li, S.; Zhang, X.; Zhu, D.; Gu, J. Feasibility of analyzing frost-damaged and non-viable maize kernels based on near infrared spectroscopy and chemometrics. *J. Cereal Sci.* **2016**, *69*, 145–150. [[CrossRef](#)]
83. Ambrose, A.; Lohumi, S.; Lee, W.-H.; Cho, B.K. Comparative nondestructive measurement of corn seed viability using Fourier transform near-infrared (FT-NIR) and Raman spectroscopy. *Sens. Actuators B Chem.* **2016**, *224*, 500–506. [[CrossRef](#)]
84. Wakholi, C.; Kandpal, L.M.; Lee, H.; Bae, H.; Park, E.; Kim, M.S.; Mo, C.; Lee, W.-H.; Cho, B.-K. Rapid assessment of corn seed viability using short wave infrared line-scan hyperspectral imaging and chemometrics. *Sens. Actuators B Chem.* **2018**, *255*, 498–507. [[CrossRef](#)]
85. Jin, B.; Qi, H.; Jia, L.; Tang, Q.; Gao, L.; Li, Z.; Zhao, G. Determination of viability and vigor of naturally-aged rice seeds using hyperspectral imaging with machine learning. *Infrared Phys. Technol.* **2022**, *122*, 104097. [[CrossRef](#)]

86. Wang, Z.; Tian, X.; Fan, S.; Zhang, C.; Li, J. Maturity determination of single maize seed by using near-infrared hyperspectral imaging coupled with comparative analysis of multiple classification models. *Infrared Phys. Technol.* **2021**, *112*, 103596. [[CrossRef](#)]
87. Zhang, L.; Sun, H.; Rao, Z.; Ji, H. Hyperspectral imaging technology combined with deep forest model to identify frost-damaged rice seeds. *Spectrochim. Acta Part A Mol. Biomol. Spectrosc.* **2020**, *229*, 117973. [[CrossRef](#)]
88. Seo, Y.-W.; Ahn, C.; Lee, H.; Park, E.; Mo, C.; Cho, B.-K. Non-Destructive Sorting Techniques for Viable Pepper (*Capsicum annuum* L.) Seeds Using Fourier Transform Near-Infrared and Raman Spectroscopy. *J. Biosyst. Eng.* **2016**, *41*, 51–59. [[CrossRef](#)]
89. Matthews, S.; Bradnock, T. The detection of seed samples of wrinkle-seeded peas (*Pisum sativum* L.) of potentially low planting value. *Proc. Int. Seed Test. Assoc.* **1976**, *32*, 553–563.
90. Yang, L.; Wen, B. Seed Quality. In *Encyclopedia of Applied Plant Sciences*, 2nd ed.; Thomas, B., Murray, B.G., Murphy, D.J., Eds.; Academic Press: Oxford, UK, 2017; pp. 553–563.
91. Gupta, N.; Chinnappa, M.; Singh, P.M.; Kumar, R.; Sagar, V. Determination of the physio-biochemical changes occurring during seed development, maturation, and desiccation tolerance in *Moringa oleifera* Lam. *S. Afr. J. Bot.* **2022**, *144*, 430–436. [[CrossRef](#)]
92. Afzal, I.; Jaffar, I.; Zahid, S.; Rehman, H.U.; Basra, S.M.A. Physiological and biochemical changes during hermetic storage of *Moringa oleifera* seeds. *S. Afr. J. Bot.* **2020**, *129*, 435–441. [[CrossRef](#)]
93. Tanaka, J.; Kiyoshi, K.; Kadokura, T.; Suzuki, K.-i.; Nakayama, S. Elucidation of the enzyme involved in 2,3,5-triphenyl tetrazolium chloride (TTC) staining activity and the relationship between TTC staining activity and fermentation profiles in *Saccharomyces cerevisiae*. *J. Biosci. Bioeng.* **2021**, *131*, 396–404. [[CrossRef](#)] [[PubMed](#)]
94. Finney, E.; Norris, K. Determination of Moisture in Corn Kernels by Near-Infrared Transmittance Measurements. *Trans. ASAE* **1978**, *21*, 0581–0584. [[CrossRef](#)]
95. Jiang, H.Y.; Zhu, Y.J.; Wei, L.; Dai, J.; Song, T.; Yan, Y.L.; Chen, S. Analysis of protein, starch and oil content of single intact kernels by near infrared reflectance spectroscopy (NIRS) in maize (*Zea mays* L.). *Plant Breed.* **2007**, *126*, 492–497. [[CrossRef](#)]
96. Esteve Agelet, L.; Ellis, D.D.; Duvick, S.; Goggi, A.S.; Hurburgh, C.R.; Gardner, C.A. Feasibility of near infrared spectroscopy for analyzing corn kernel damage and viability of soybean and corn kernels. *J. Cereal Sci.* **2012**, *55*, 160–165. [[CrossRef](#)]
97. Wang, Y.; Peng, Y.; Zhuang, Q.; Zhao, X. Feasibility analysis of NIR for detecting sweet corn seeds vigor. *J. Cereal Sci.* **2020**, *93*, 102977. [[CrossRef](#)]
98. Mukasa, P.; Wakholi, C.; Mo, C.; Oh, M.; Joo, H.-J.; Suh, H.K.; Cho, B.-K. Determination of viability of *Retinispora* (*Hinoki cypress*) seeds using FT-NIR spectroscopy. *Infrared Phys. Technol.* **2019**, *98*, 62–68. [[CrossRef](#)]
99. Ma, T.; Tsuchikawa, S.; Inagaki, T. Rapid and non-destructive seed viability prediction using near-infrared hyperspectral imaging coupled with a deep learning approach. *Comput. Electron. Agric.* **2020**, *177*, 105683. [[CrossRef](#)]
100. Pang, L.; Wang, L.; Yuan, P.; Yan, L.; Yang, Q.; Xiao, J. Feasibility study on identifying seed viability of *Sophora japonica* with optimized deep neural network and hyperspectral imaging. *Comput. Electron. Agric.* **2021**, *190*, 106426. [[CrossRef](#)]
101. Pang, L.; Men, S.; Yan, L.; Xiao, J. Rapid Vitality Estimation and Prediction of Corn Seeds Based on Spectra and Images Using Deep Learning and Hyperspectral Imaging Techniques. *IEEE Access* **2020**, *8*, 123026–123036. [[CrossRef](#)]
102. Zhang, J.; Dai, L.; Cheng, F. Identification of Corn Seeds with Different Freezing Damage Degree Based on Hyperspectral Reflectance Imaging and Deep Learning Method. *Food Anal. Methods* **2021**, *14*, 389–400. [[CrossRef](#)]
103. Feng, L.; Zhu, S.; Zhang, C.; Bao, Y.; Feng, X.; He, Y. Identification of Maize Kernel Vigor under Different Accelerated Aging Times Using Hyperspectral Imaging. *Molecules* **2018**, *23*, 3078. [[CrossRef](#)] [[PubMed](#)]
104. Dainty, J.C. Introduction. In *Laser Speckle and Related Phenomena*; Dainty, J.C., Ed.; Springer: Berlin/Heidelberg, Germany, 1975; pp. 1–7.
105. Singh, P.; Chatterjee, A.; Rajput, L.S.; Rana, S.; Kumar, S.; Nataraj, V.; Bhatia, V.; Prakash, S. Development of an intelligent laser biospeckle system for early detection and classification of soybean seeds infected with seed-borne fungal pathogen (*Colletotrichum truncatum*). *Biosyst. Eng.* **2021**, *212*, 442–457. [[CrossRef](#)]
106. Sutton, D.B.; Punja, Z.K. Investigating biospeckle laser analysis as a diagnostic method to assess sprouting damage in wheat seeds. *Comput. Electron. Agric.* **2017**, *141*, 238–247. [[CrossRef](#)]
107. Rahmanian, A.; Mireei, S.A.; Sadri, S.; Gholami, M.; Nazeri, M. Application of biospeckle laser imaging for early detection of chilling and freezing disorders in orange. *Postharvest Biol. Technol.* **2020**, *162*, 111118. [[CrossRef](#)]
108. Toderi, M.A.; Riquelme, B.D.; Galizzi, G.E. An experimental approach to study the red blood cell dynamics in a capillary tube by biospeckle laser. *Opt. Lasers Eng.* **2020**, *127*, 105943. [[CrossRef](#)]
109. Singh, P.; Chatterjee, A.; Bhatia, V.; Prakash, S. Application of laser biospeckle analysis for assessment of seed priming treatments. *Comput. Electron. Agric.* **2020**, *169*, 105212. [[CrossRef](#)]
110. Braga, R.A.; Dal Fabbro, I.M.; Borem, F.M.; Rabelo, G.; Arizaga, R.; Rabal, H.J.; Trivi, M. Assessment of Seed Viability by Laser Speckle Techniques. *Biosyst. Eng.* **2003**, *86*, 287–294. [[CrossRef](#)]
111. Passoni, I.; Dai Pra, A.; Rabal, H.; Trivi, M.; Arizaga, R. Dynamic speckle processing using wavelets based entropy. *Opt. Commun.* **2005**, *246*, 219–228. [[CrossRef](#)]
112. Dai Pra, A.L.; Passoni, L.I.; Rabal, H. Evaluation of laser dynamic speckle signals applying granular computing. *Signal Process.* **2009**, *89*, 266–274. [[CrossRef](#)]
113. Braga, R.A.; Cardoso, R.R.; Bezerra, P.S.; Wouters, F.; Sampaio, G.R.; Varaschin, M.S. Biospeckle numerical values over spectral image maps of activity. *Opt. Commun.* **2012**, *285*, 553–561. [[CrossRef](#)]

114. Thakur, P.S.; Tiwari, B.; Kumar, A.; Gedam, B.; Bhatia, V.; Krejcar, O.; Dobrovolny, M.; Nebhen, J.; Prakash, S. Deep transfer learning based photonics sensor for assessment of seed-quality. *Comput. Electron. Agric.* **2022**, *196*, 106891. [[CrossRef](#)]
115. Rivera, F.P.; Braga, R.A.; Iannetta, P.; Toorop, P. Sound as a qualitative index of speckle laser to monitor biological systems. *Comput. Electron. Agric.* **2019**, *158*, 271–277. [[CrossRef](#)]
116. Thakur, P.S.; Chatterjee, A.; Rajput, L.S.; Rana, S.; Bhatia, V.; Prakash, S. Laser biospeckle technique for characterizing the impact of temperature and initial moisture content on seed germination. *Opt. Lasers Eng.* **2022**, *153*, 106999. [[CrossRef](#)]
117. Cardoso, R.R.; Costa, A.G.; Nobre, C.M.B.; Braga, R.A. Frequency signature of water activity by biospeckle laser. *Opt. Commun.* **2011**, *284*, 2131–2136. [[CrossRef](#)]
118. Al-Hammad, B.A.; Al-Ammari, B.S. Seed viability of five wild Saudi Arabian species by germination and X-ray tests. *Saudi J. Biol. Sci.* **2017**, *24*, 1424–1429. [[CrossRef](#)] [[PubMed](#)]
119. Ahmed, M.R.; Yasmin, J.; Collins, W.; Cho, B.-K. X-ray CT image analysis for morphology of muskmelon seed in relation to germination. *Biosyst. Eng.* **2018**, *175*, 183–193. [[CrossRef](#)]
120. Ahmed, M.R.; Yasmin, J.; Wakholi, C.; Mukasa, P.; Cho, B.-K. Classification of pepper seed quality based on internal structure using X-ray CT imaging. *Comput. Electron. Agric.* **2020**, *179*, 105839. [[CrossRef](#)]
121. Liu, X.; Gao, C.; Xing, D. A non-invasive and rapid seed vigor biosensor based on quantitative measurement of superoxide generated by aleurone cell in intact seeds. *Biosens. Bioelectron.* **2009**, *24*, 1537–1542. [[CrossRef](#)]
122. Ornellas, F.L.S.; de Sousa, A.O.; Pirovani, C.P.; Araújo, M.N.; da Costa, D.S.; Dantas, B.F.; Barbosa, R.M. Gene expression, biochemical and physiological activities in evaluating melon seed vigor through ethanol release. *Sci. Hortic.* **2020**, *261*, 108884. [[CrossRef](#)]
123. Daneshvar, A.; Tigabu, M.; Karimidoost, A.; Odén, P.C. Flotation techniques to improve viability of *Juniperus polycarpus* seed lots. *J. For. Res.* **2017**, *28*, 231–239. [[CrossRef](#)]
124. Demelash, L.; Tigabu, M.; Oden, P.C. Separation of empty and dead-filled seeds from a seed lot of *Pinus Patula* with IDS technique. *Seed Sci. Technol.* **2002**, *30*, 677–681.
125. Demelash, L.; Tigabu, M.; Oden, P.C. Enhancing germinability of *Schinus molle* L. seed lot from Ethiopia with specific gravity and IDS techniques. *New For.* **2003**, *26*, 33–41. [[CrossRef](#)]
126. Hendeniya, N.; Sandanuwan, T.; Amarasinghe, D.A.S.; Attygalle, D.; Weragoda, S.C.; Ranaweera, B.; Rathnayake, K.; Lalanka, M. Atmospheric Pressure Plasma Treatment as a Cost-Effective and Eco-Friendly Pre-Treatment Method to Enhance Seed Performance in Germination and Early Seedling Growth. In Proceedings of the 2021 Moratuwa Engineering Research Conference (MERCon), Moratuwa, Sri Lanka, 27–29 July 2021; pp. 643–648.
127. Jorge, M.H.A.; Ray, D.T. Germination characterization of guayule seed by morphology, mass and, X-ray analysis. *Ind. Crops Prod.* **2005**, *22*, 59–63. [[CrossRef](#)]
128. Lin, H.; Man, Z.-x.; Kang, W.-c.; Guan, B.-b.; Chen, Q.-s.; Xue, Z.-l. A novel colorimetric sensor array based on boron-dipyrromethene dyes for monitoring the storage time of rice. *Food Chem.* **2018**, *268*, 300–306. [[CrossRef](#)]

**Disclaimer/Publisher's Note:** The statements, opinions and data contained in all publications are solely those of the individual author(s) and contributor(s) and not of MDPI and/or the editor(s). MDPI and/or the editor(s) disclaim responsibility for any injury to people or property resulting from any ideas, methods, instructions or products referred to in the content.